

Profiling of Inlet Ports of Z-Engine

Final report

Dr. Vladimir Zenkin

Dr. Andrey Kuleshov

AUMET OY - 2012

1. Content

1. Content	2
2. Specification	3
3. Boundary conditions	4
4. Profiling of axisymmetric part of the port	5
5. Profiling of intake port in the cylinder head.....	18
6. Discharge coefficient for thermodynamic engine simulation	30
7. Thermodynamic z-engine simulation with obtained intake port discharge coefficient	32
8. Conclusion	36
9. References.....	38
Appendix	37

2. Specification

A target of the research is an optimisation of the inside shape of the z-engine intake port in order to obtain a maximal mass flow at 3600 rpm. Simulations was carried out with thermodynamic code DIESEL-RK [1] and CFD code NSF-3 developed in Moscow Bauman State Technical University. The NSF code uses truncated cells to form a sophisticated shape of a spatial domain. This technique allows usage cube cells in the space being not contacted with walls, and near-wall cells being the cubes without cut off parts, fig. 1. The computing procedure is very economical because:

- implicit algorithm is quite stable: one make one iteration per time step with Courant criterion about $Co \approx 0.3 \div 0.4$ [2].

- the same algorithm is used for both kinds of cells: full and truncated.

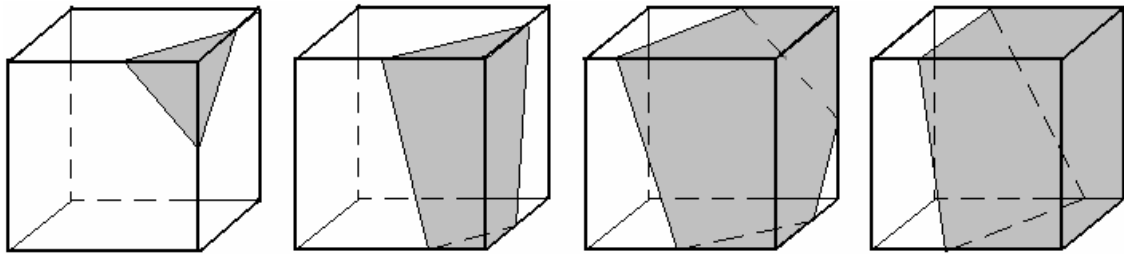


Fig. 1. The cube cells without cut off parts, being used for description of sophisticated shape of a spatial domain.

Before simulation the NSF code was verified by comparison of the results with results obtained with Star-CD and CFX codes as well with experimental data.

Engine and intake valve data:

- 2 intake valves per cylinder;
- cylinder bore: 72 mm,
- piston stroke : 70 mm,
- rated (nominal) valve lift where mass flow is maximal: $L_V = 4$ mm;
- face diameter – 25-28 mm,
- face angle – 30 deg;
- maximum valve head diameter : $D_V = 28$ mm.

3. Boundary conditions

Maximum mass flow through intake ports corresponds to the point 301 deg of CA (fig. 2).

Intake Manifold Pressure: $p_{int} = 16.6$ bar

Intake Manifold Temperature: $T_{int} = 310$ K

Cylinder Pressure: $p_{cyl} = 9.9$ bar

These data were obtained from previous thermodynamic z-engine simulation and optimization at maximum power point. The simulation with DIESEL-RK [1] has shown the insufficient fresh charge in the cylinder at high capacity point. So, this point parameters were selected as boundary conditions for current research. During all CFD simulations there static flow conditions was modelled.

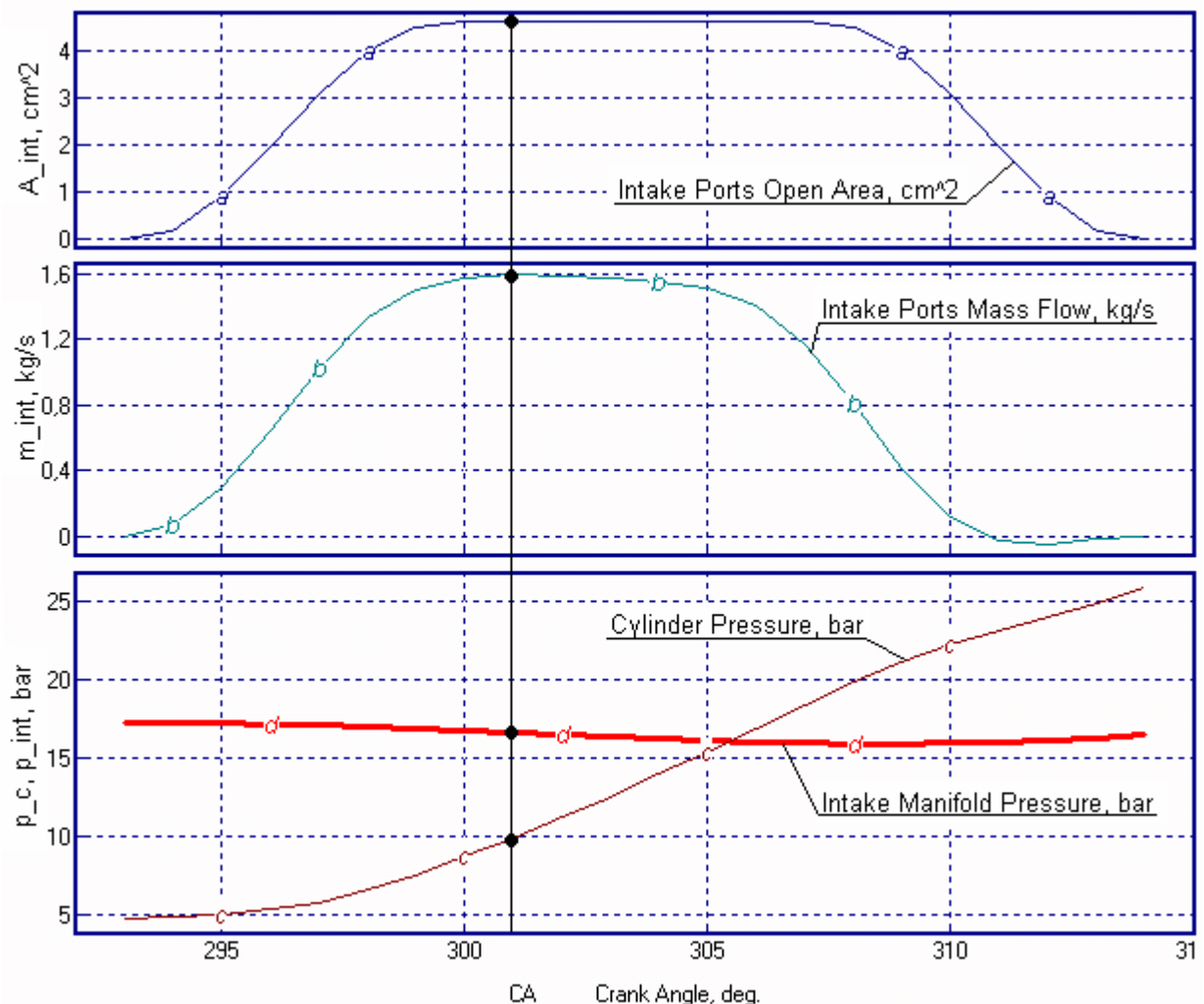


Fig 2. Intake process parameters simulated with DIESEL-RK

4. Profiling of axisymmetric part of the port

As a first step of port shape optimization there was selected an optimization of axisymmetric part of the port in the region of intake valve seat. The independent optimization of this element of port allows bound a number of cells in the mesh and use a quite fine mesh. Last allows perform simulations faster and with good accuracy. The sketch of axisymmetric part of the port and 3D model of this part are presented in fig. 3, 4. In the fig. 3 there are shown the main dimensions being optimized with parametrical research technique. These dimensions are:

- Throat diameter, D_t ;
- Minimum throat diameter position, h_t ;
- Confuser angle, α_c ;
- Radius R_v ;
- Valve head diameter, D_v .

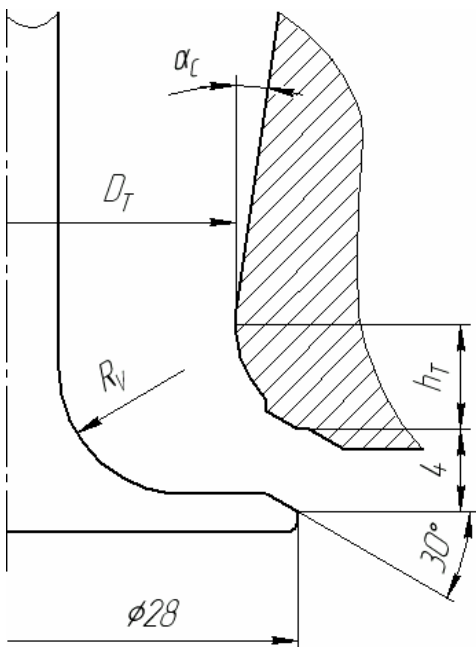


Fig. 3. Sketch of axisymmetric part of the port

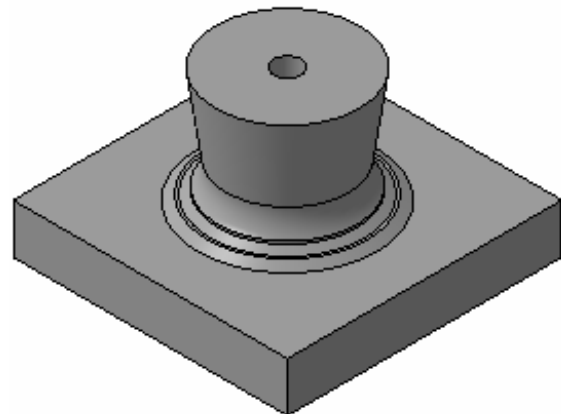


Fig. 4. 3D-model of the computational domain

At the simulation of the flow in the axisymmetrical part of the port there was used mesh with ~250 000 cells. Mesh in the cylinder head port had about 350 000 cells. In both researches the turbulence was modelled by usage a turbulence viscosity $\mu_T = 0.01$ Pa·s.

At the discharge coefficient estimations there was used a mesh with ~ 1000 000 cells and k- ϵ model of turbulence.

Effect of the throat diameter D_t on a port mass air flow is presented in the fig .5. The Mach number fields illustrate drop down of the flow if $D_t < 20$ mm due to throat diameter starts to be critical section where sonic velocity takes place. Normally at the supersonic pressure ratio the sonic flow should be in the valve gap (in the seat) as it shown in the right picture of fig. 5. The optimum value of D_t is 22 mm. This value was preferred to have in reserve of port flow area for the case if valve lift will exceed 4 mm. This value of D_t was fixed in future researches.

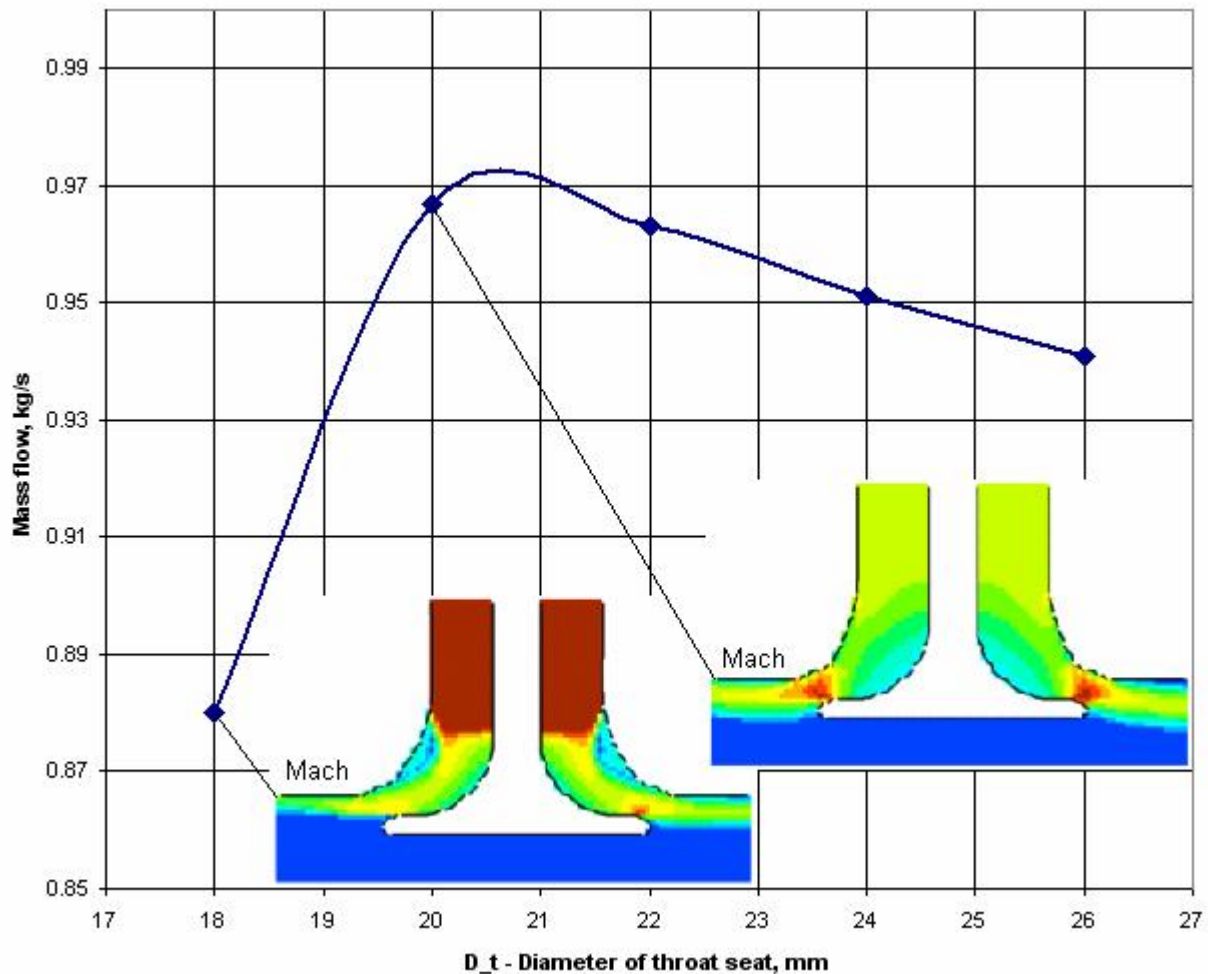


Fig. 5. Effect of the throat diameter D_t on the ports mass flow

The calculated fields of velocities, Mach number, static pressure and total pressure are presented in the figures 6, 7, 8, 9 for different values of throat diameter D_t .

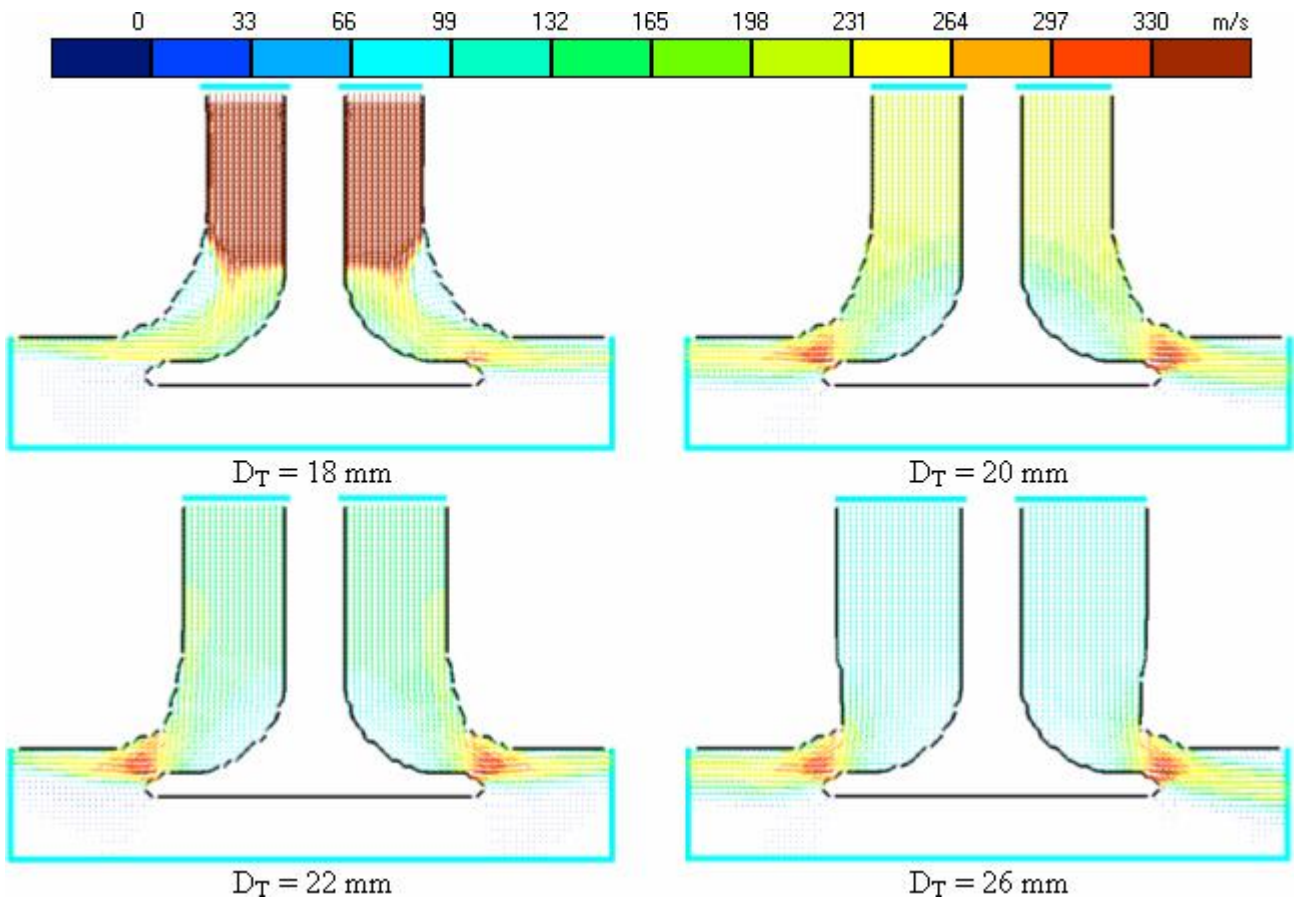


Fig. 6. The velocity field at different diameter of throat seat

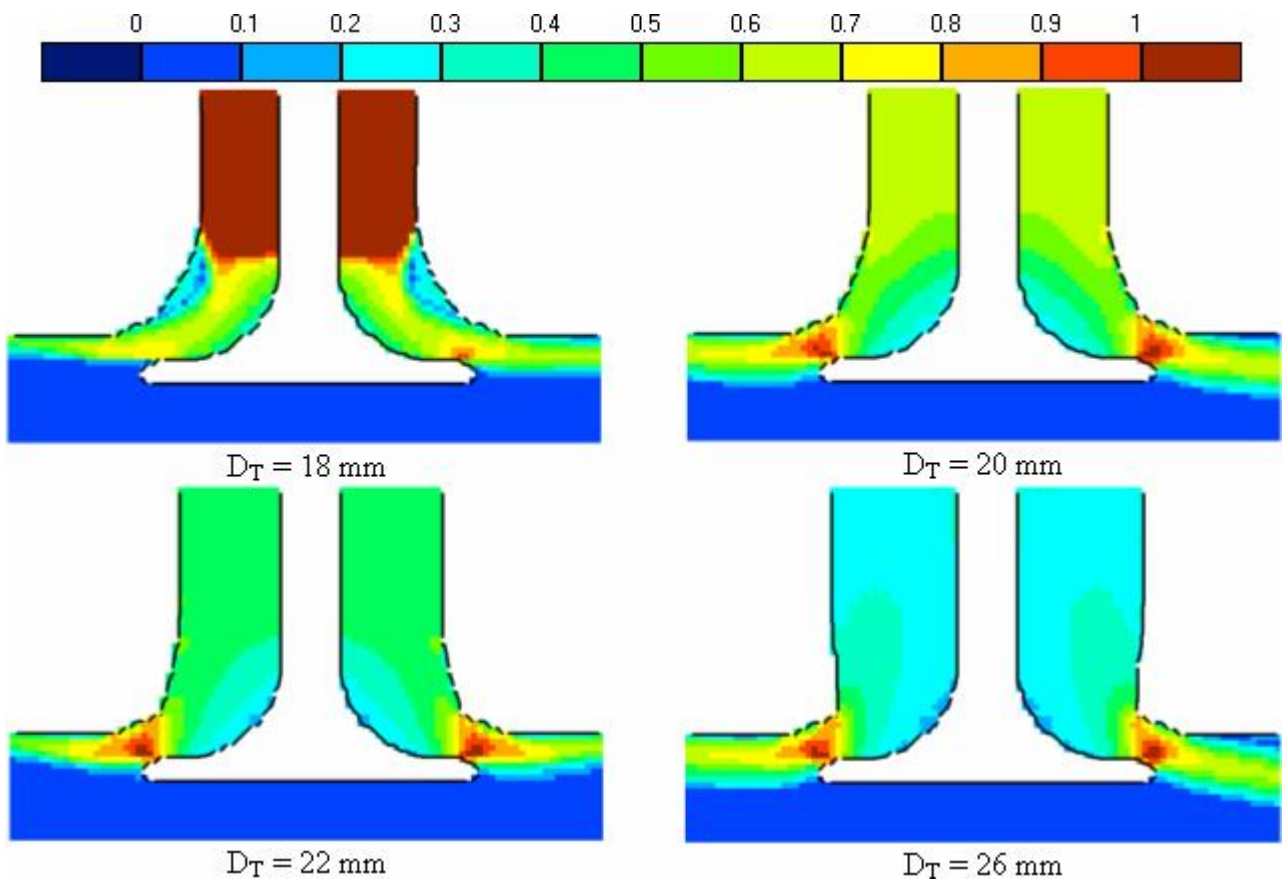


Fig. 7. The Mach number field at different diameter of throat seat

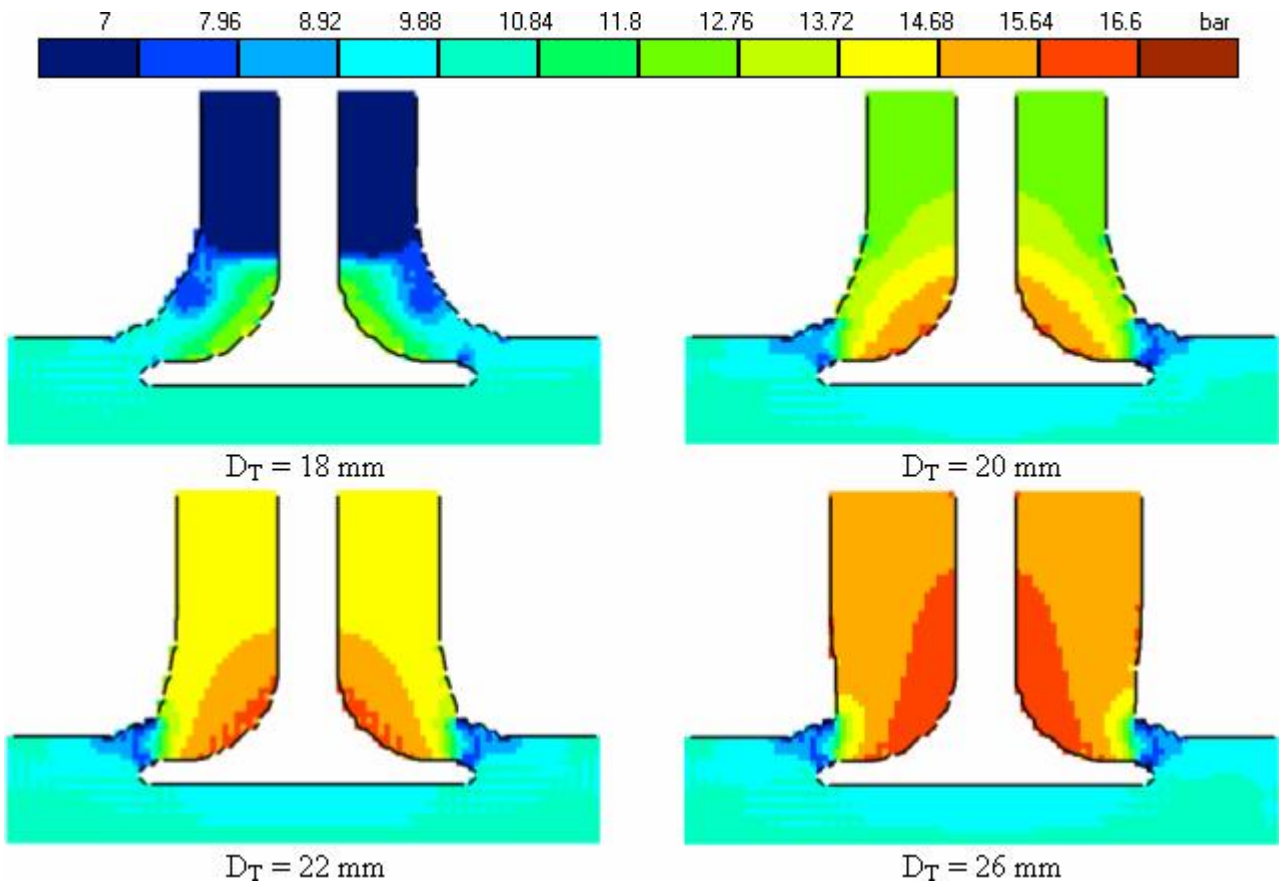


Fig. 8. The static pressure field at different diameter of throat seat

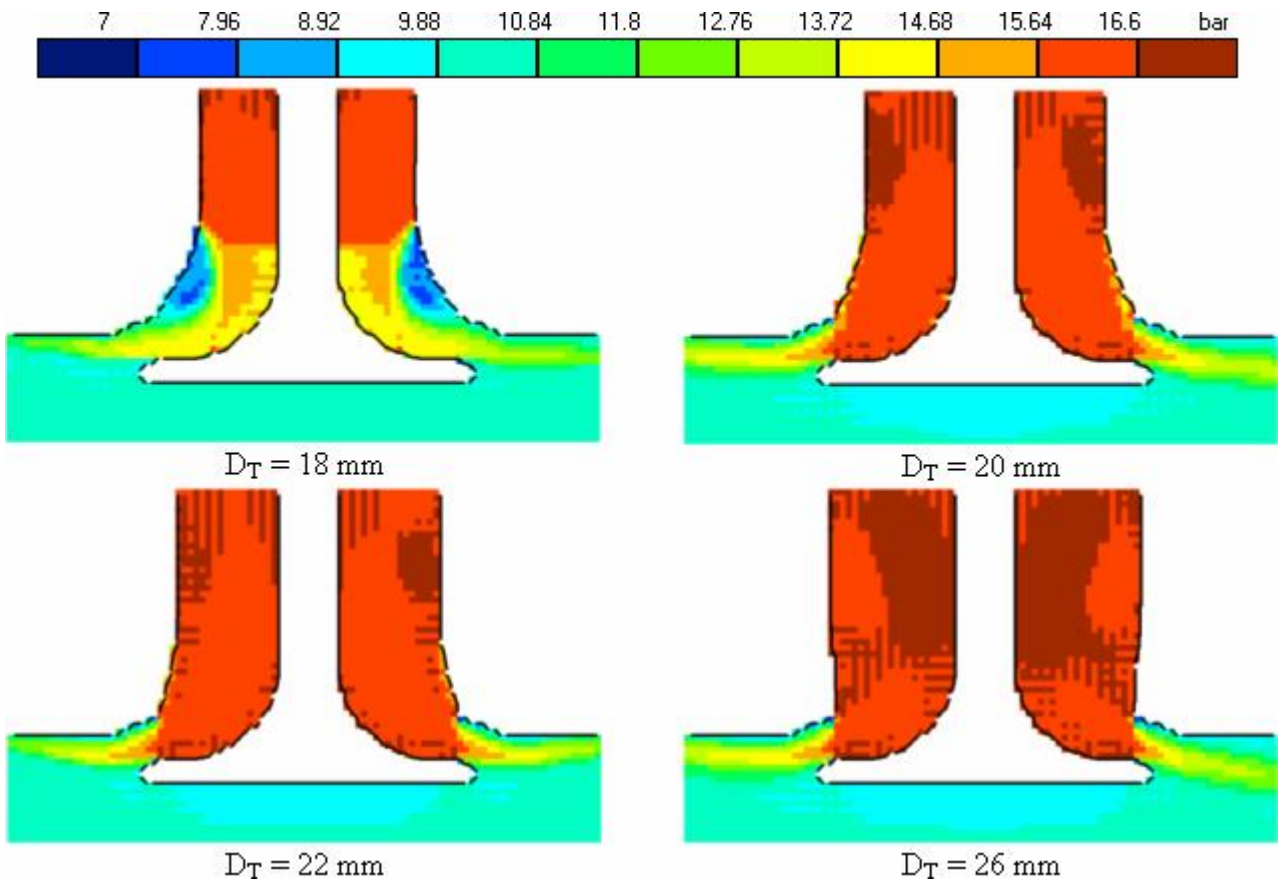


Fig. 9. The total pressure field at different diameter of throat seat

Effect of small valve radius is presented in the fig. 10. This effect may be explained by improvement of the flow condition in the region of valve seat having 30° angle of inclination. However small radius decreases strength and durability of the valve, so, this parameters should be estimated and selected on the base of strength simulation. Here the was accepted $R_v = 6$ mm.

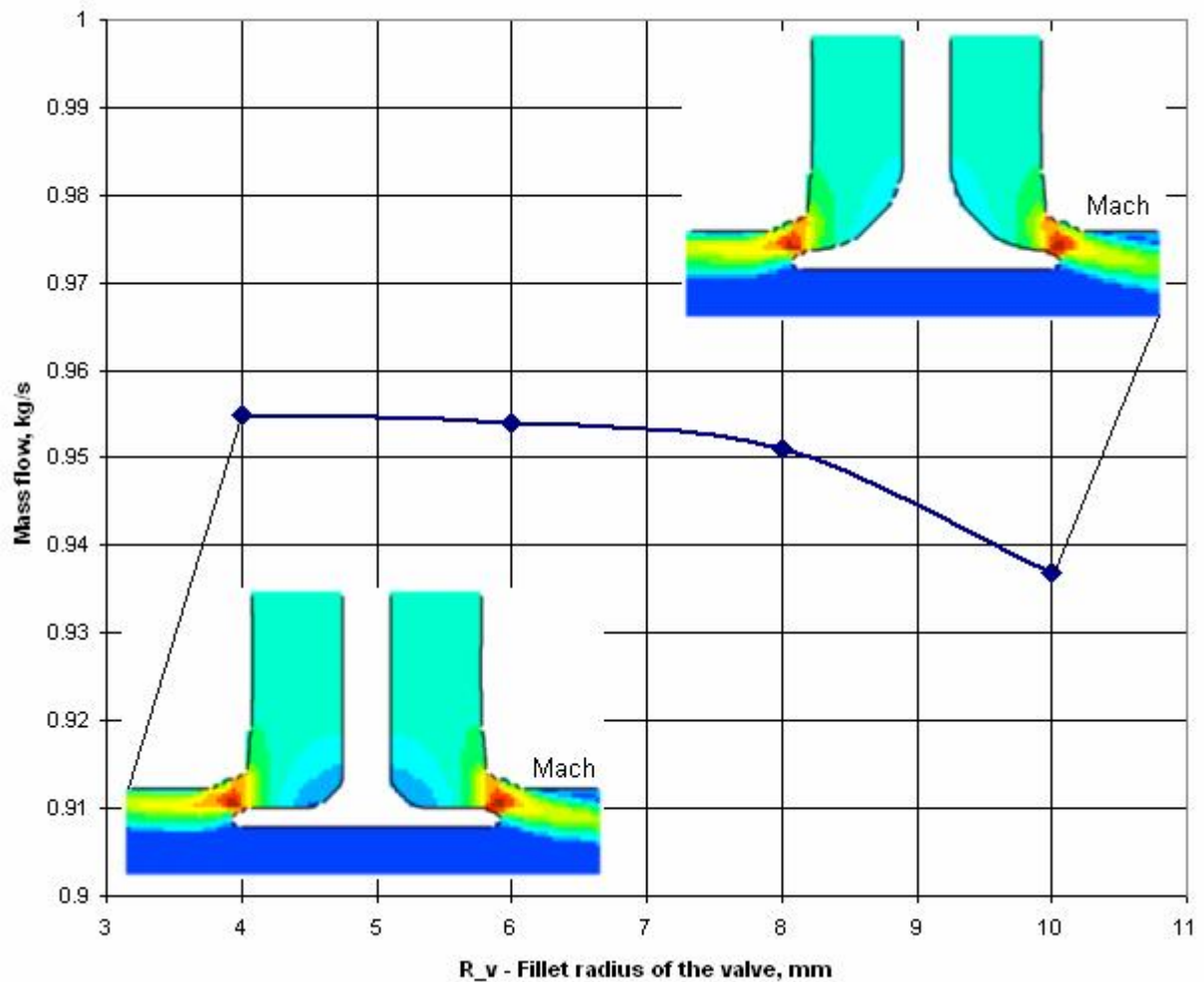


Fig. 10. Effect of valve radius R_v on the mass flow of the intake valves.

The calculated fields of velocities, Mach number, static pressure and total pressure are presented in the figures 11, 12, 13, 14 for different values of radius R_v .

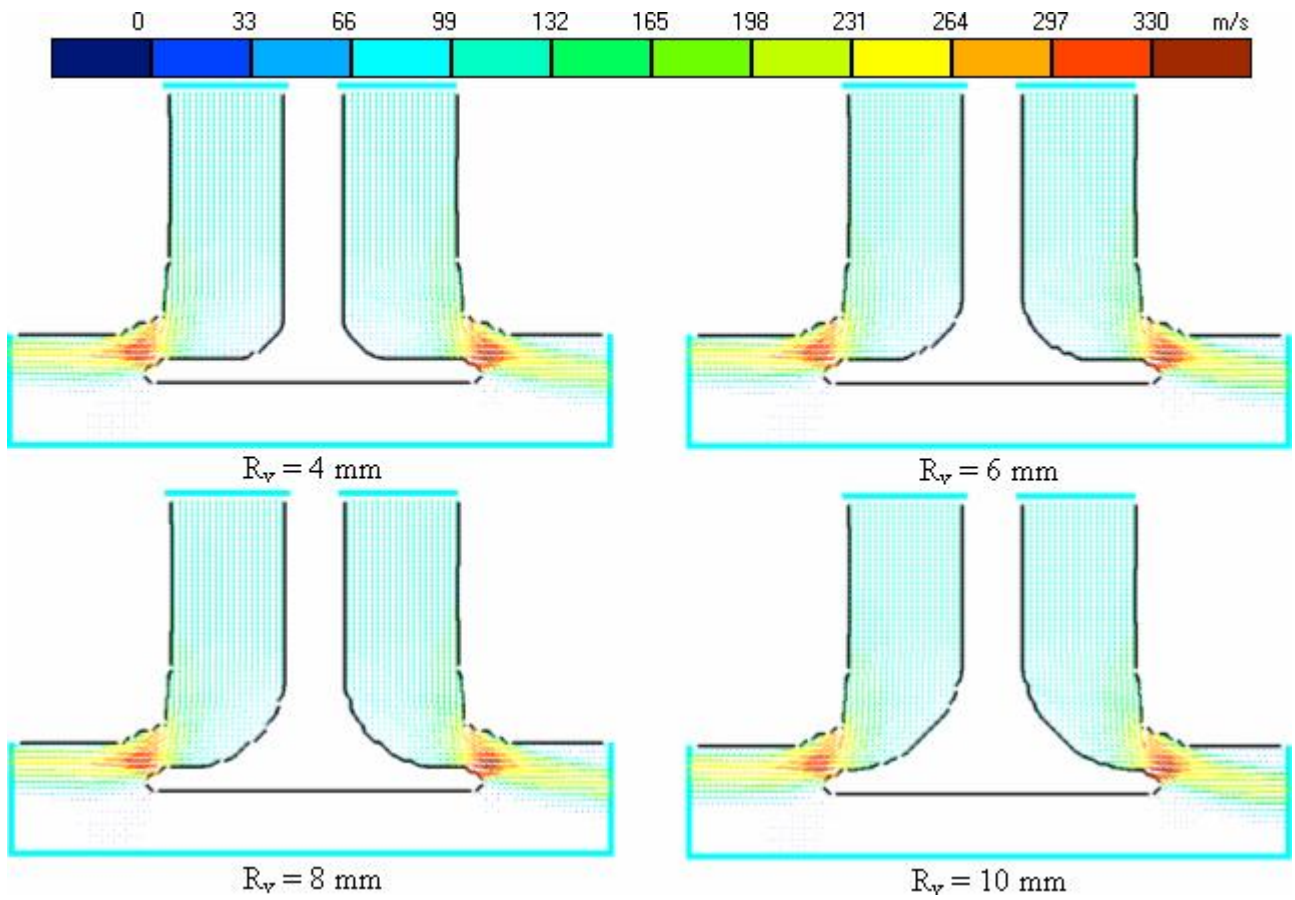


Fig. 11. The velocity field at different fillet radius of the valve

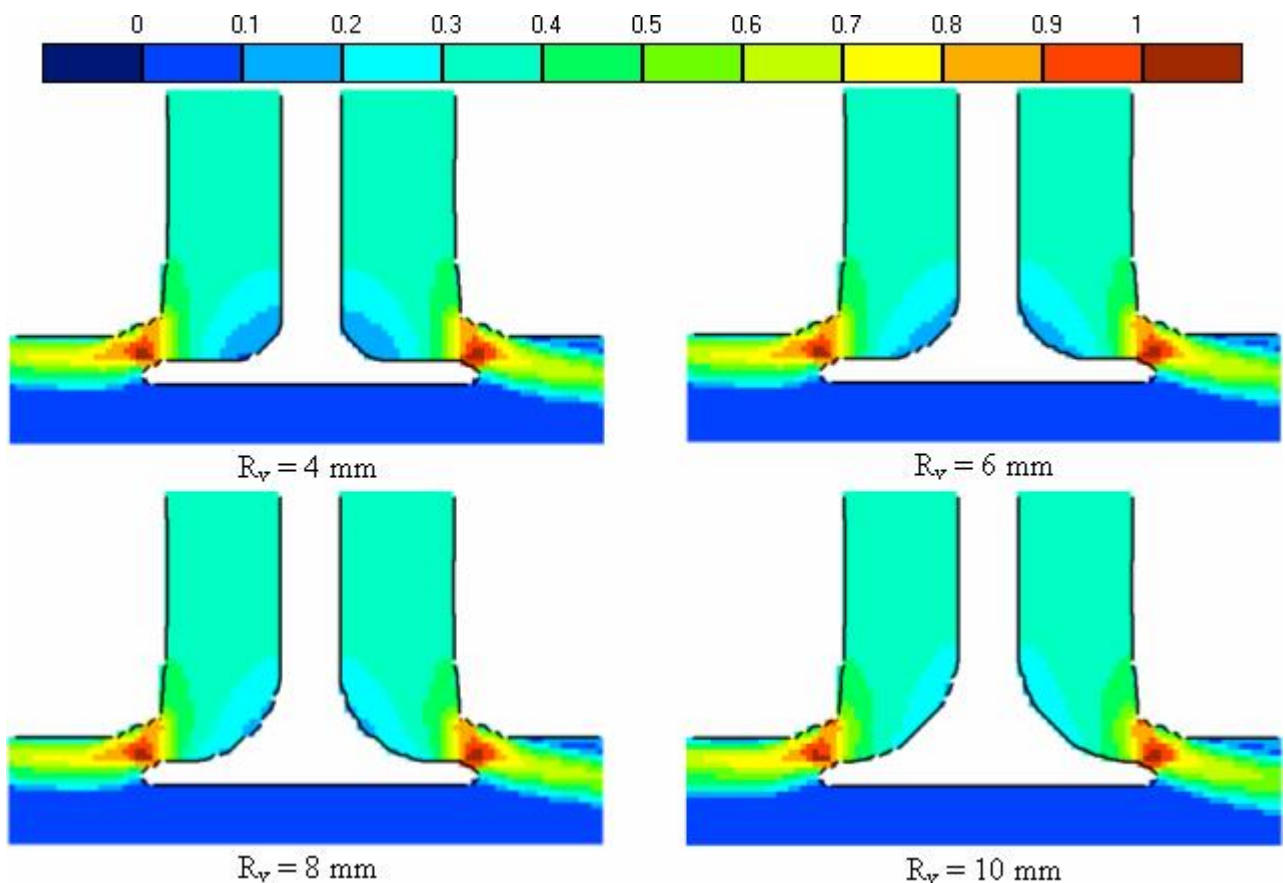


Fig. 12. The Mach number field at different fillet radius of the valve

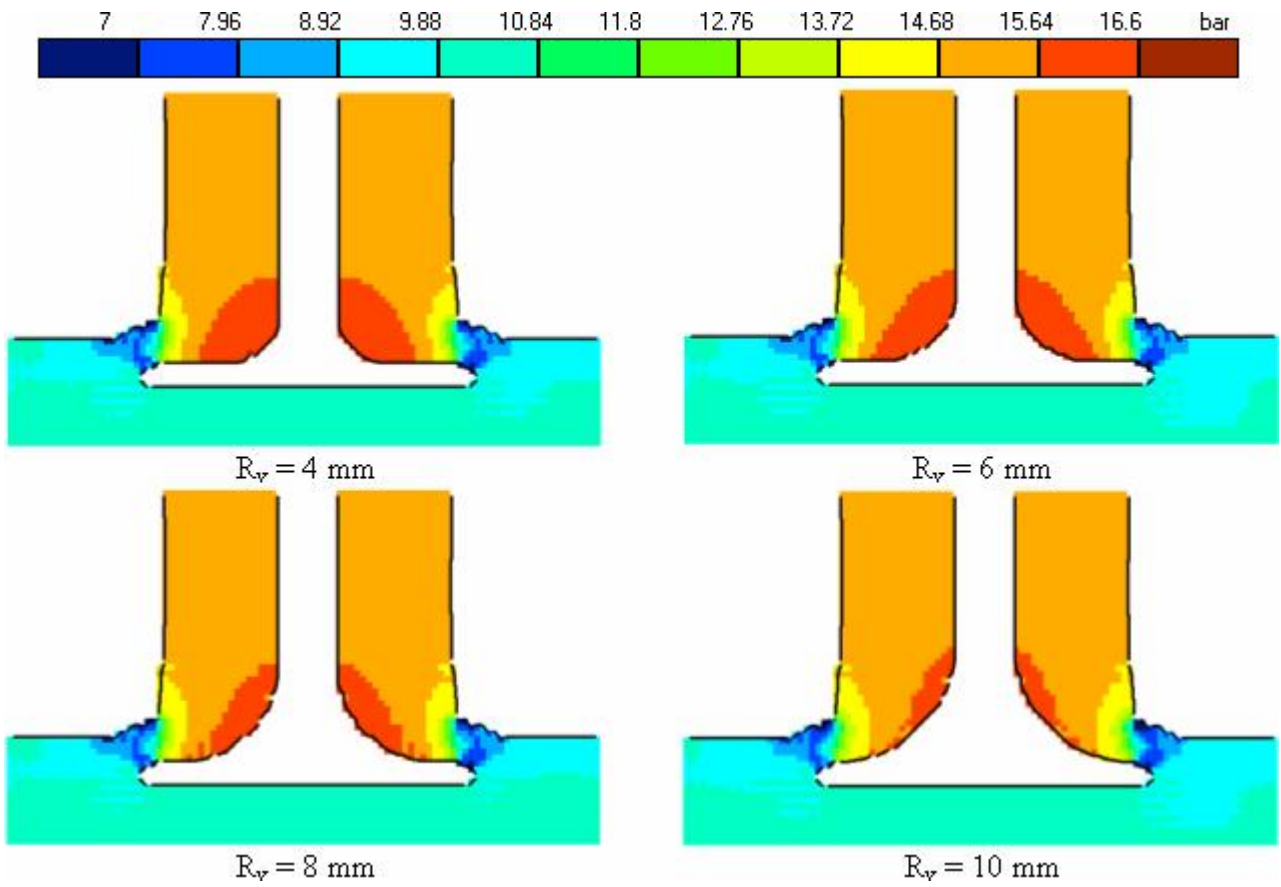


Fig. 13. The static pressure field at different fillet radius of the valve

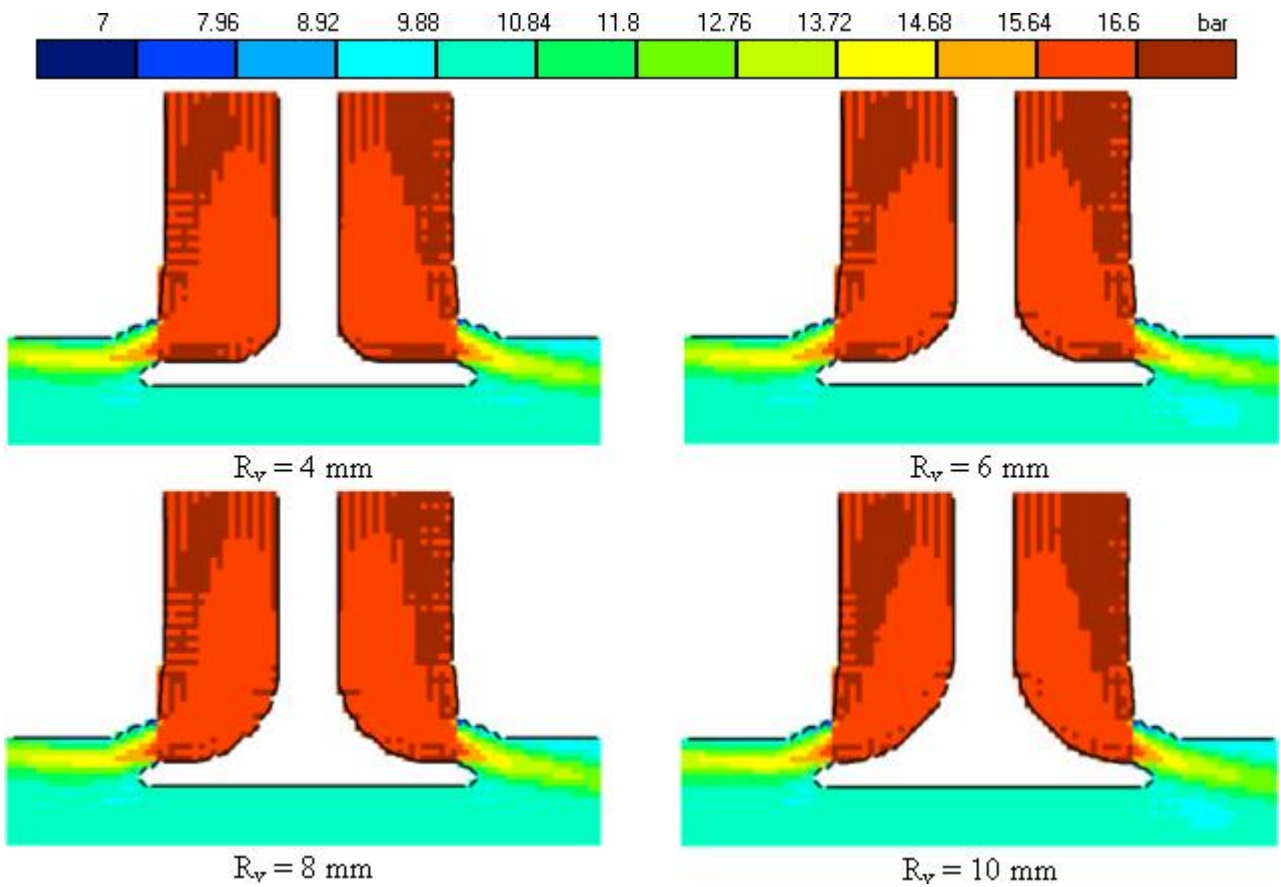


Fig. 14. The total pressure field at different fillet radius of the valve

The effect of port throat position h_t on air mass flow is not large, fig. 15. If throat is too close to a seat there is a tearing off zone of flow appeared due to a small radius between throat and seat surface (fig. 16,17, $h_t = 3$ mm). If throat is too far from the seat it decrease the radius of port turn and result in another tearing off zone due to sharp bend of the flow before axisymmetric part of the port. As a result of the research the $h_t = 5$ mm was accepted.

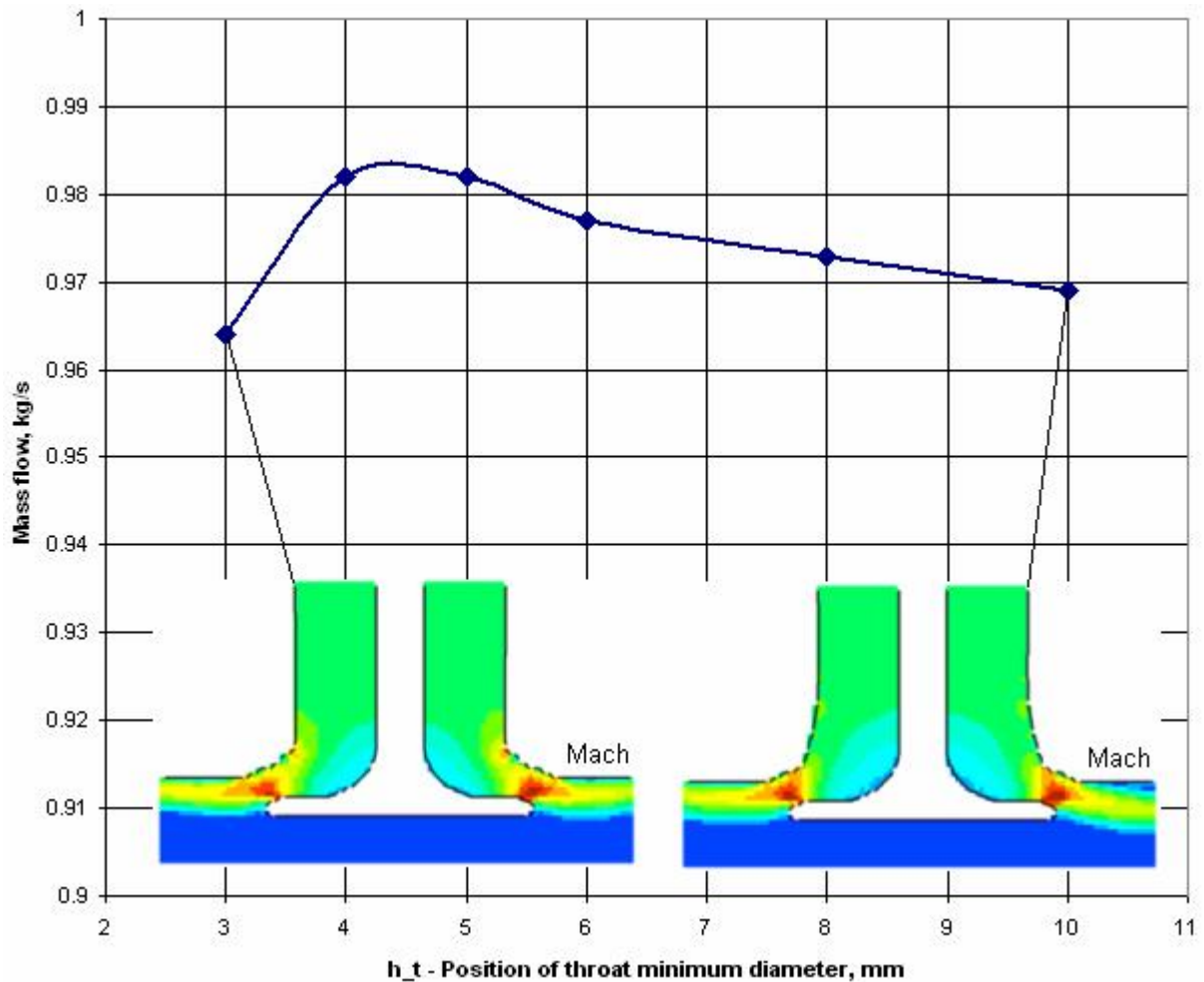


Fig. 15. Dependence of the mass flow on the position of throat minimum diameter

The calculated fields of velocities, Mach number, static pressure and total pressure are presented in the figures 16, 17, 18, 19 for different values of port throat position h_t

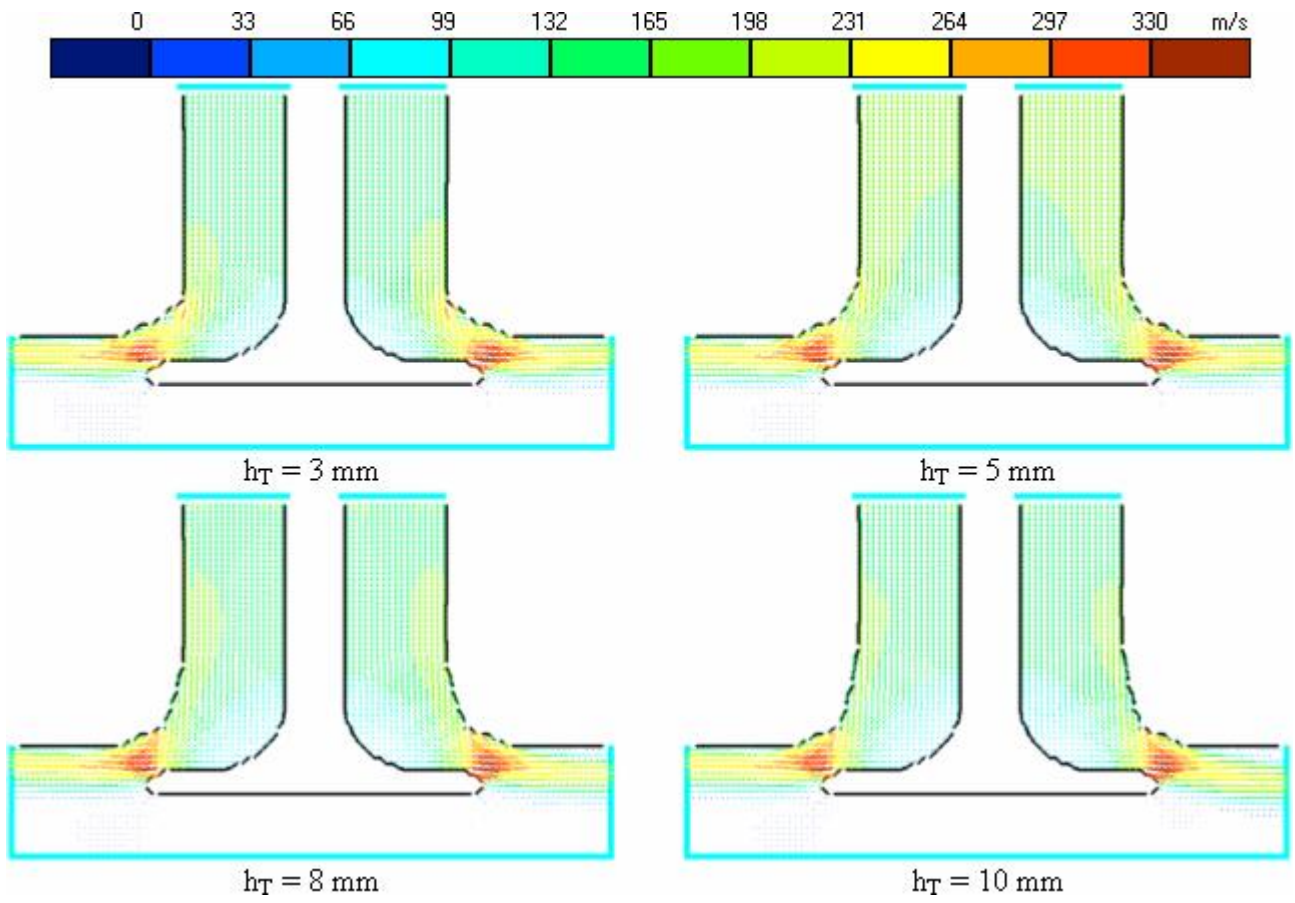


Fig. 16. The velocity field at different position of throat minimum diameter h_t

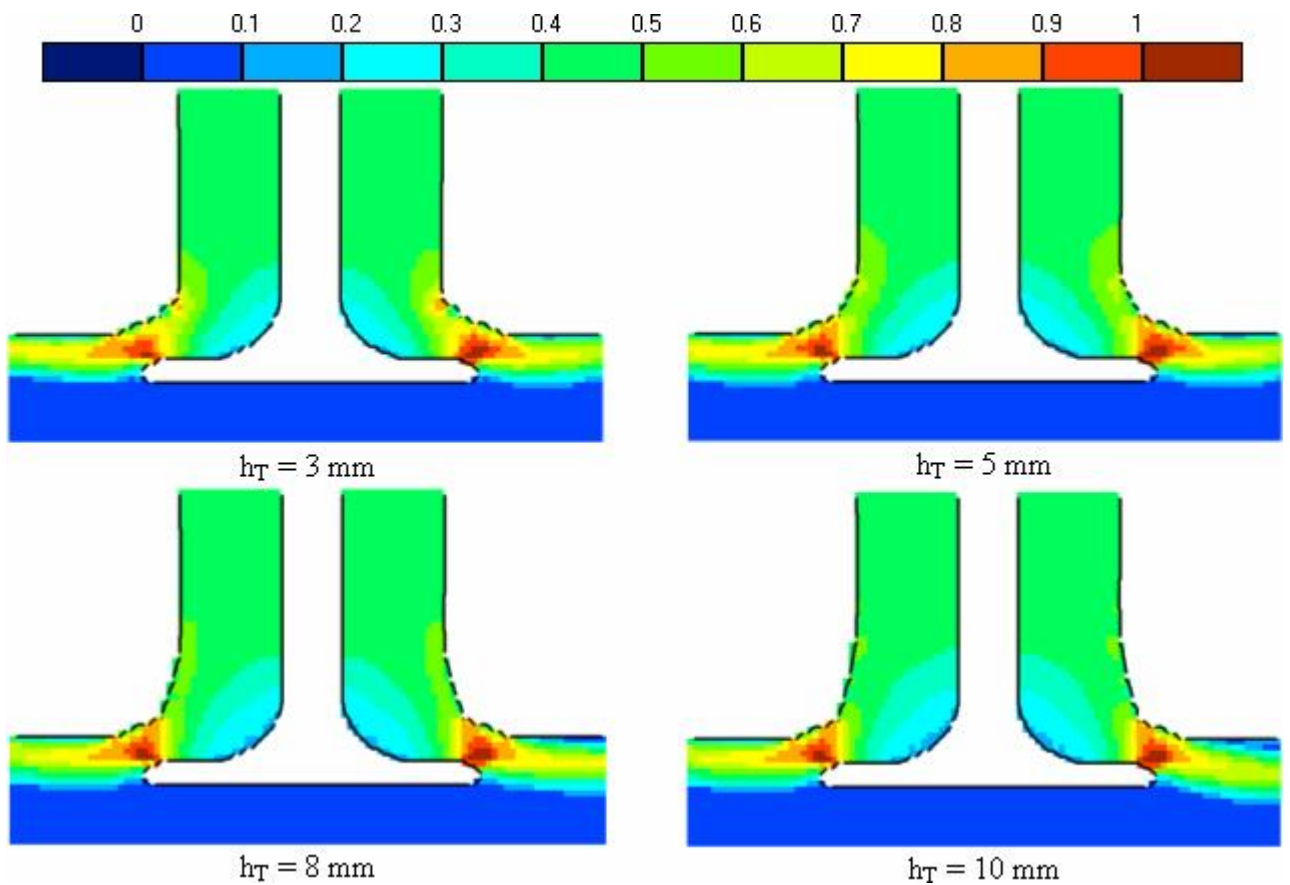


Fig. 17. The Mach number field at different position of throat minimum diameter h_t

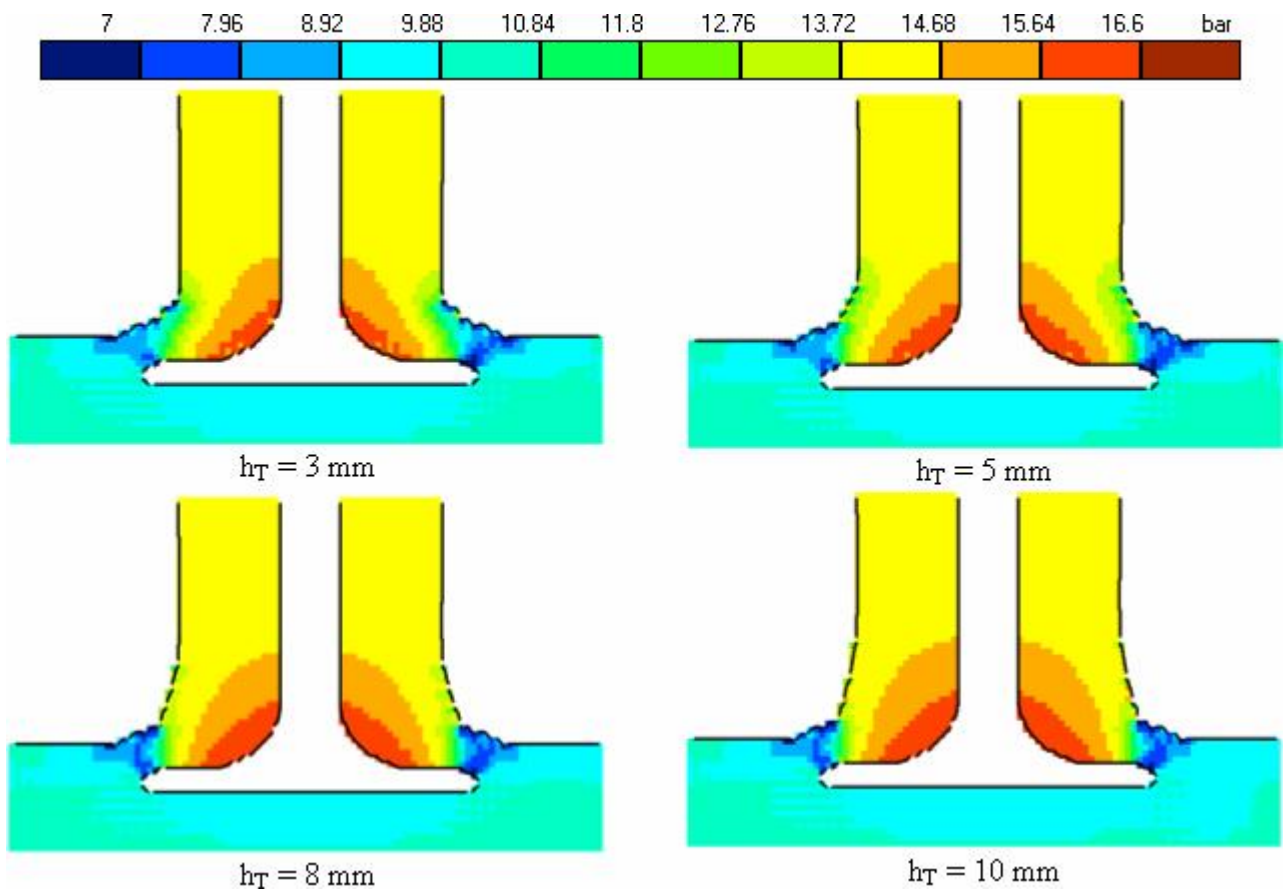


Fig. 18. The static pressure field at different position of throat minimum diameter h_t

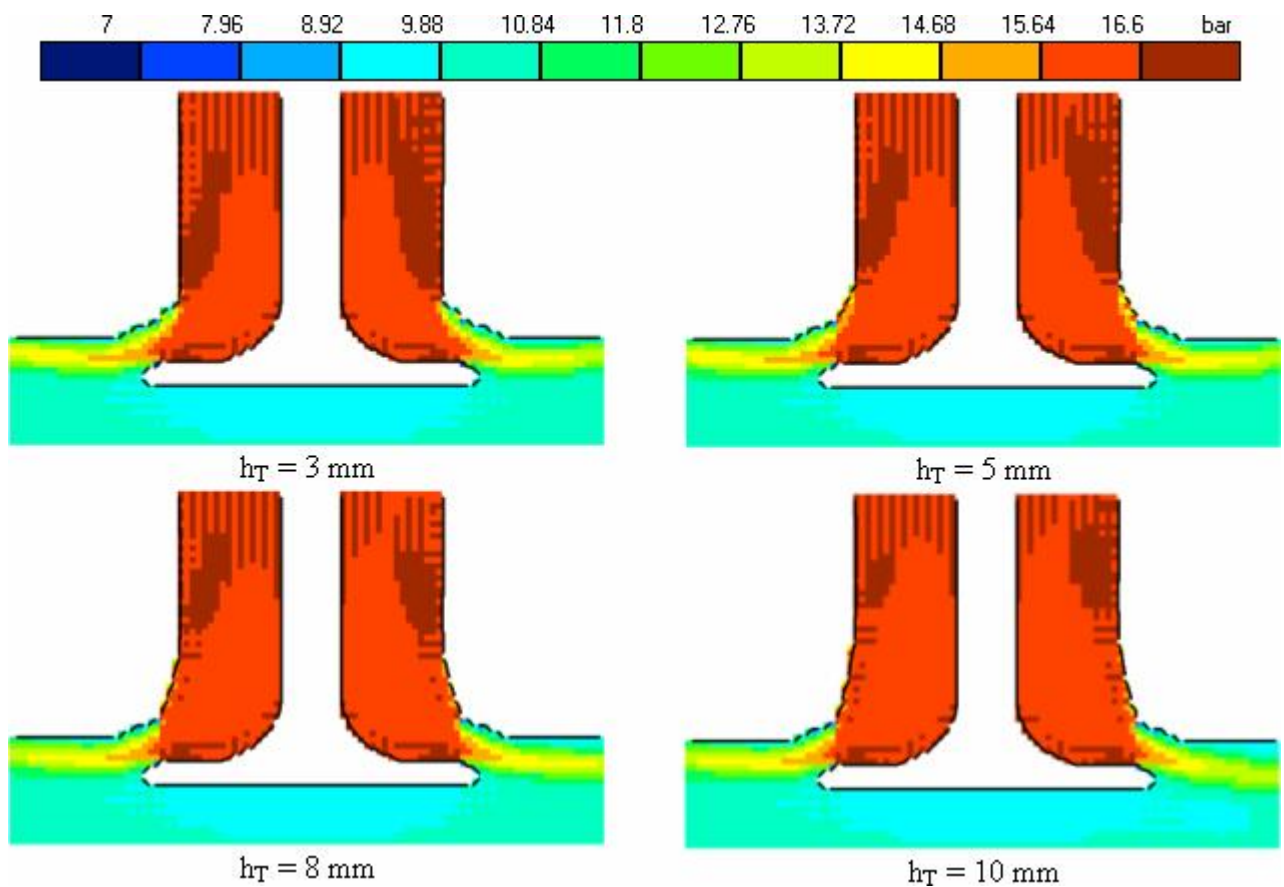


Fig. 19. The total pressure field at different position of throat minimum diameter h_t

The effect of Confuser angle α_c on air mass flow is very small, fig. 20. It is well known the confuser flow has not hydraulic losses.

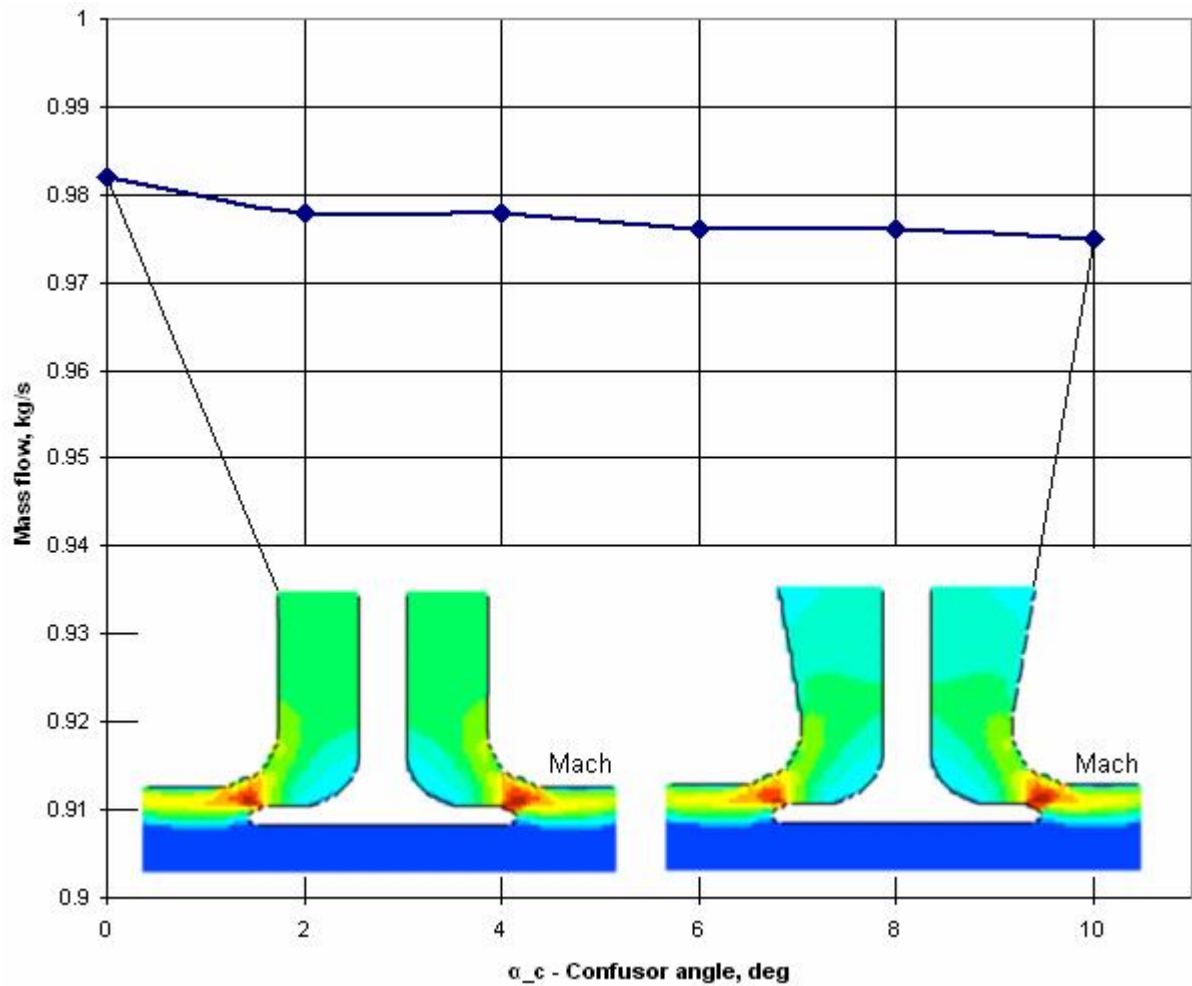


Fig. 20. Dependence of the mass flow on the confuser angle α_c

The calculated fields of velocities, Mach number, static pressure and total pressure are presented in the figures 21, 22, 23, 24 for different values of the confuser angle α_c

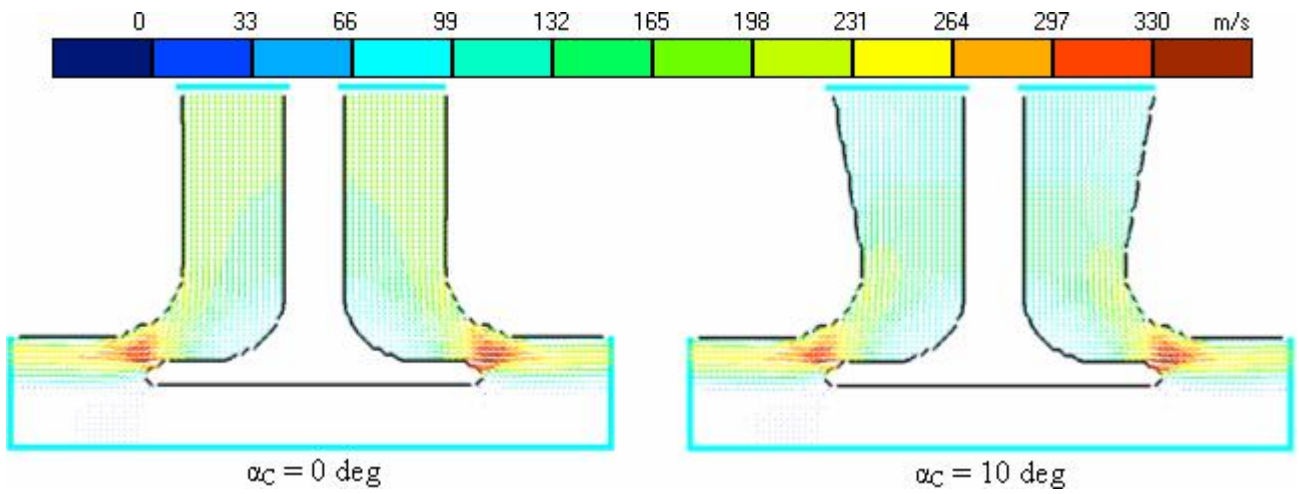


Fig. 21. The velocity field at different confuser angle a_c

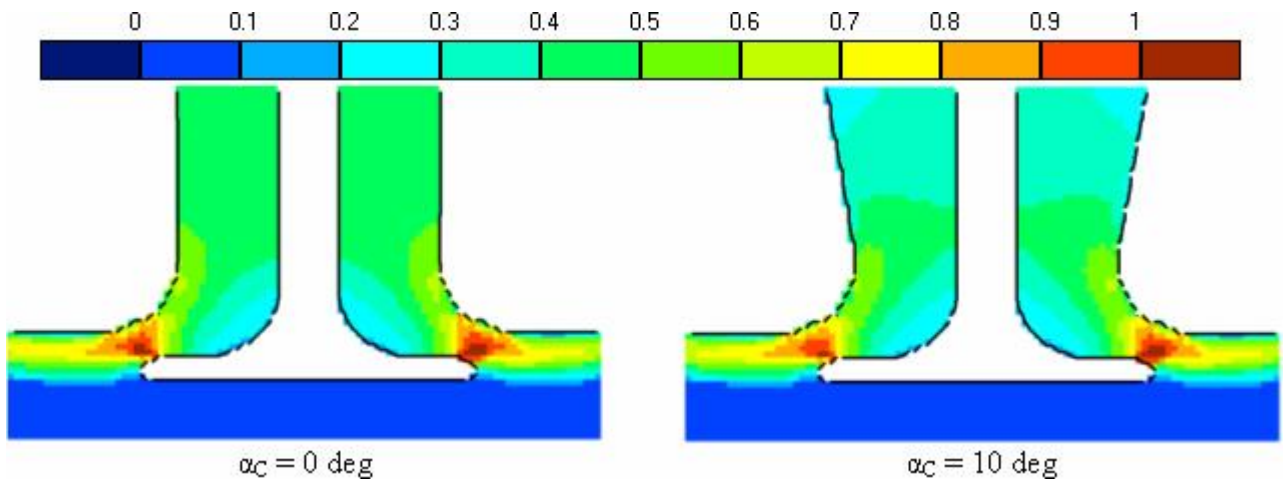


Fig. 22. The Mach number field at different confuser angle a_c

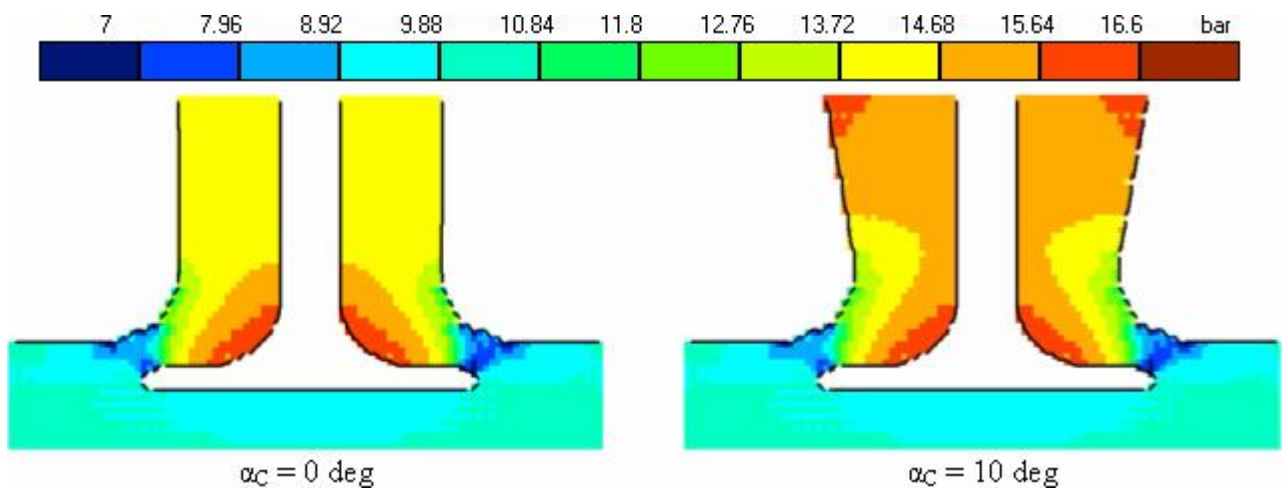


Fig. 23. The static pressure field at different confuser angle a_c

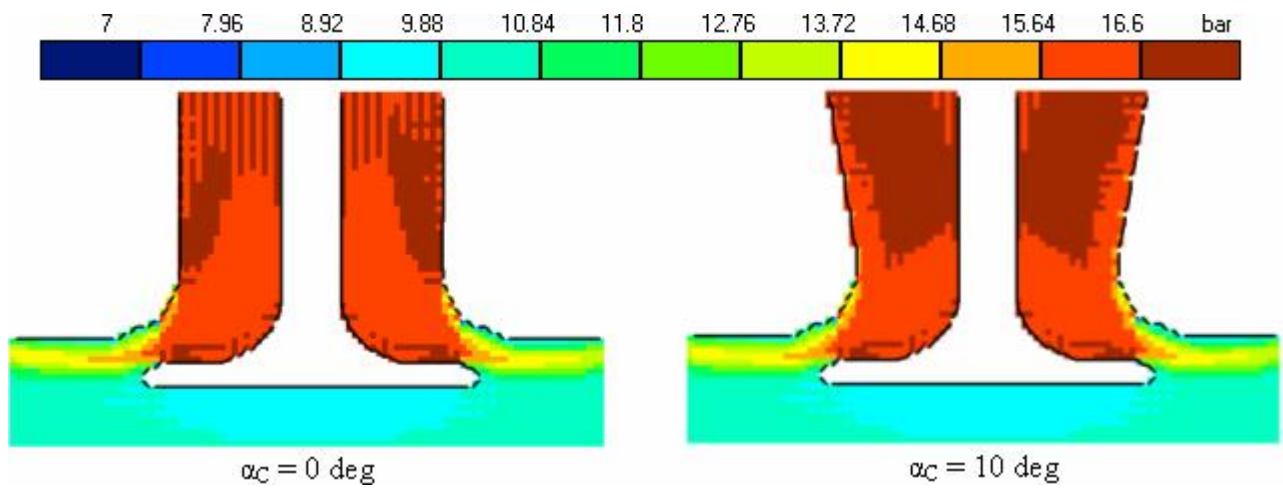


Fig. 24. The total pressure field at different confuser angle α_c

Conclusion: in the result of presented research the following design of axisymmetric part of the port was accepted (fig. 25) and fixed for future steps of the research.

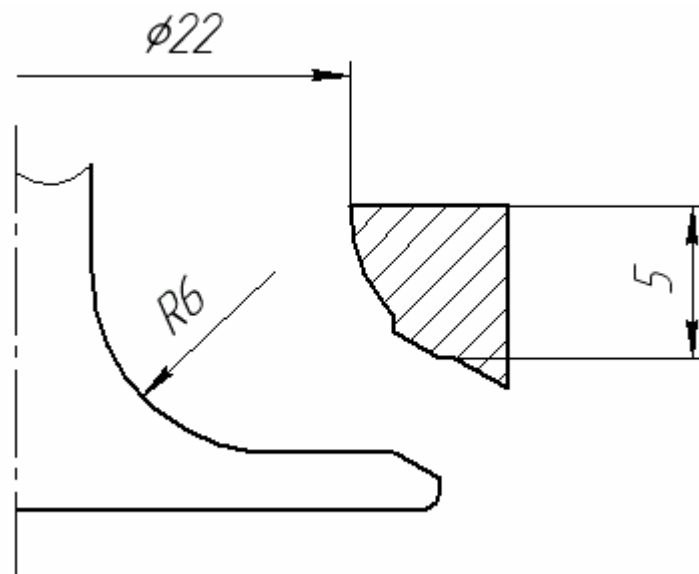


Fig. 25. Sketch of the recommended axisymmetric part of the port

5. Profiling of intake port in the cylinder head

The port design parameters being investigated at the current stage of the research are presented in the fig. 26.

There was optimized:

- Shape of port inlet (oval or circular).
- Position of the upper edge of the port roof, h_{max} (from 55 up to 64 mm).
- Cross section area of the port inlet A_{INL} (from 8 up to 18 cm²).
- Valve head diameter D_v (from 25 up to 28 mm).
- Distance from cylinder axis to the plane of the intake valves axis X_v (from 7 up to 13 mm)

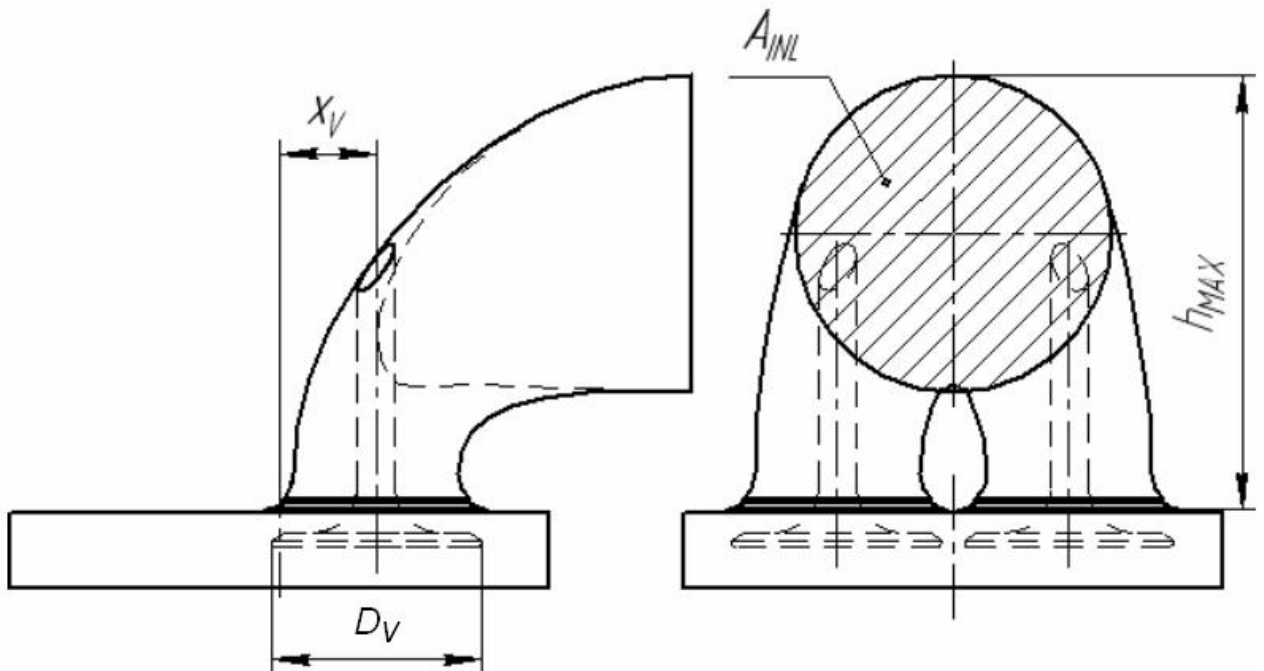


Fig. 26. Sketch of intake port in the cylinder head

A comparison of calculated mass air flow of ports having oval cross section of inlet (fig. 27) and circular cross section of inlet (fig. 27) are the same. Therefore, for further consideration has been selected port with a circular cross section, as the simpler in construction.

The calculated fields of velocities, Mach number, static pressure and total pressure are presented in the figure 29 for different variants of intake port inlet design.

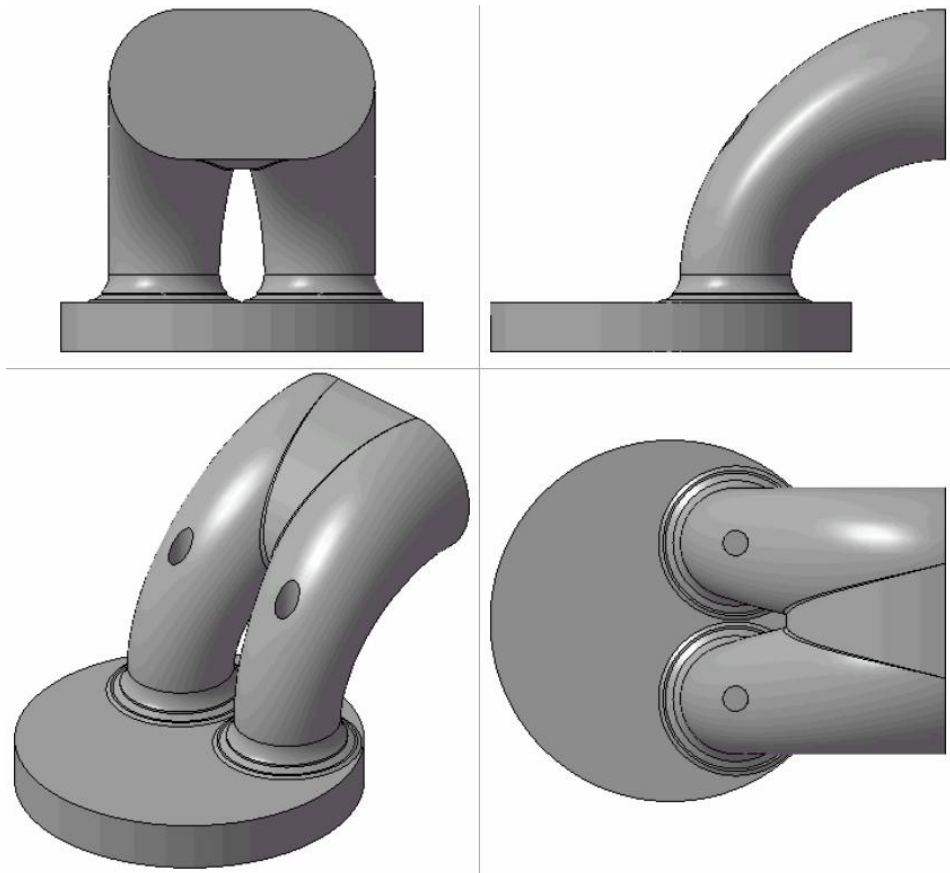


Fig. 27. Port with oval inlet

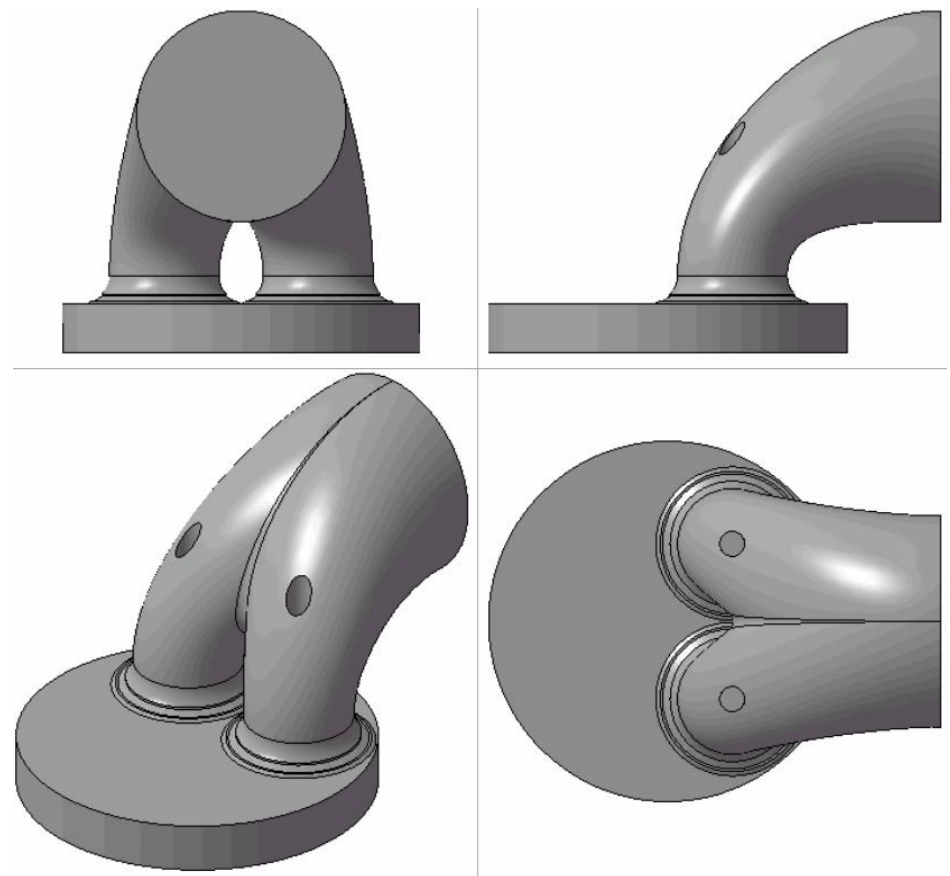


Fig. 28. Port with circular inlet

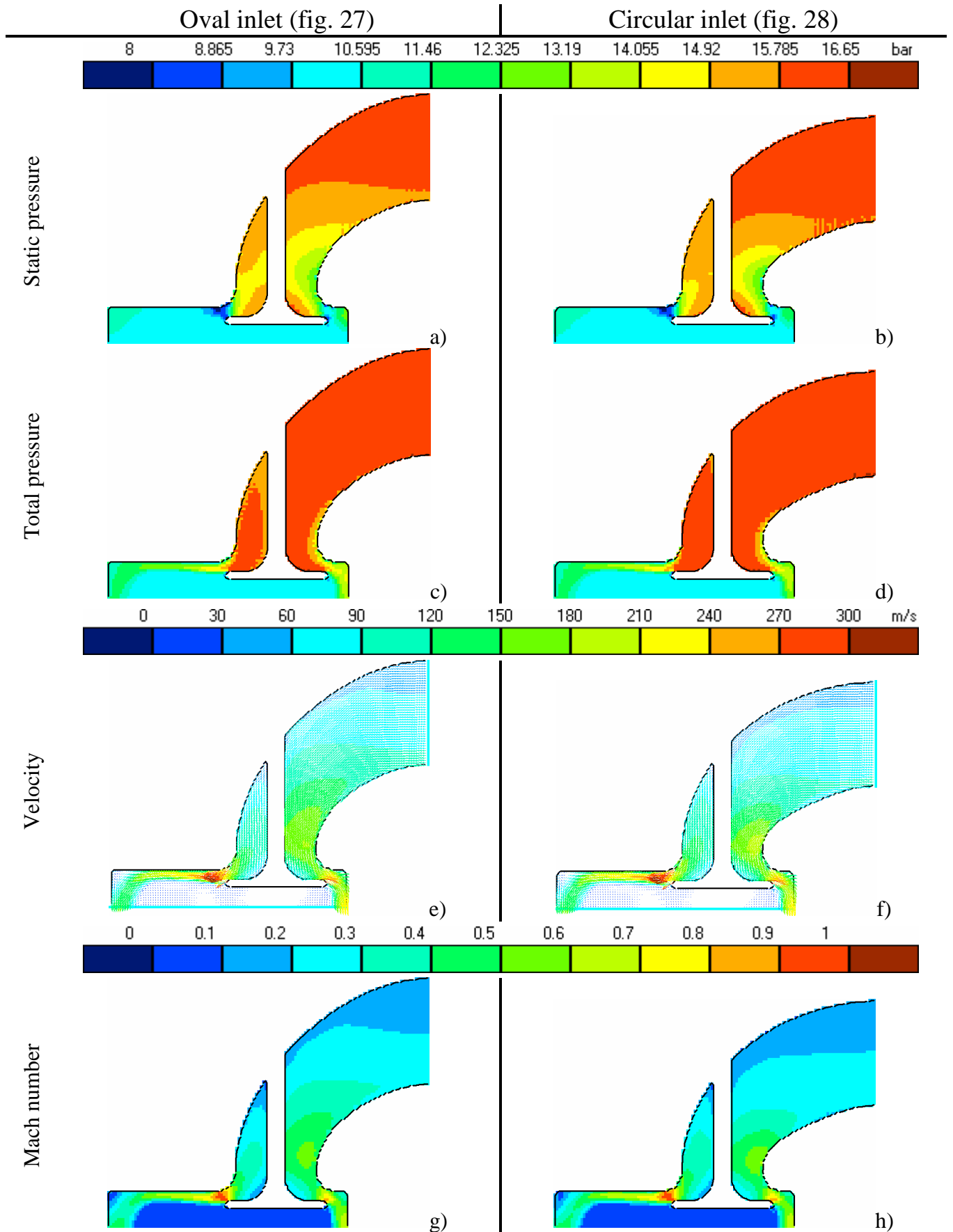


Fig. 29. Gas flow parameters for Oval and Circular port inlets

Two variants of port inlet design was tested, fig. 30.

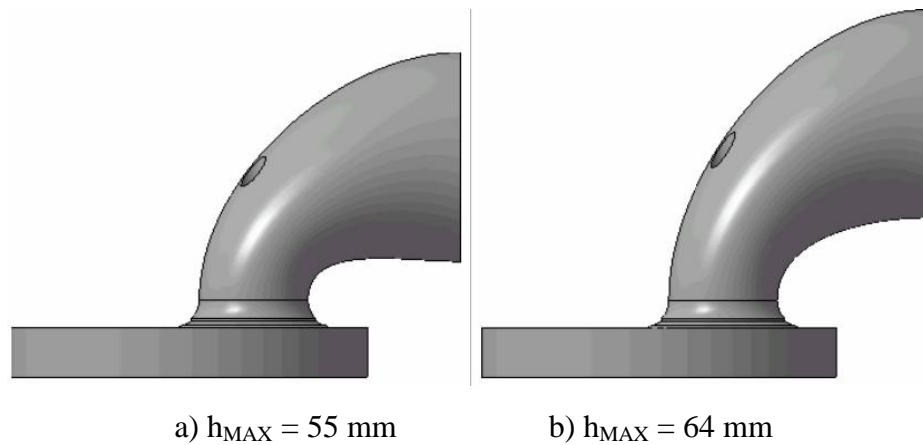


Fig. 30. Intake port at different position of the upper edge of the port roof

Usually a large height of the intake port inlet h_{max} (fig. 26) helps to reach a smooth bend of a port and more equable (even) velocity field. However, here the simulations have shown the flow tearing off zone at small $h_{max} = 55$ mm is only slightly larger than one in the case of large $h_{max} = 64$ mm, fig. 31, 32 e, 32 f. The variation of mass flow at changing h_{max} is not large, so it was allowed for the further research $h_{max} = 58$ mm. In practice this dimension should be obtained from general design requirements.

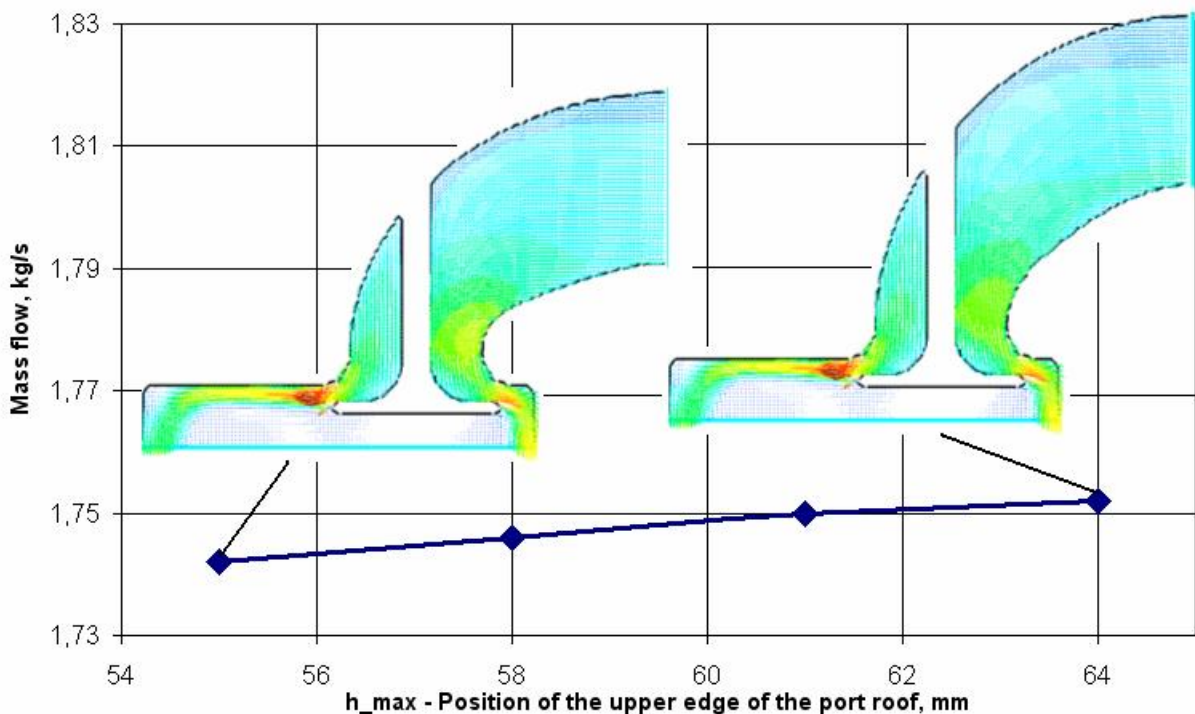


Fig. 31. Effect of the position of the upper edge of the port roof on the mass flow

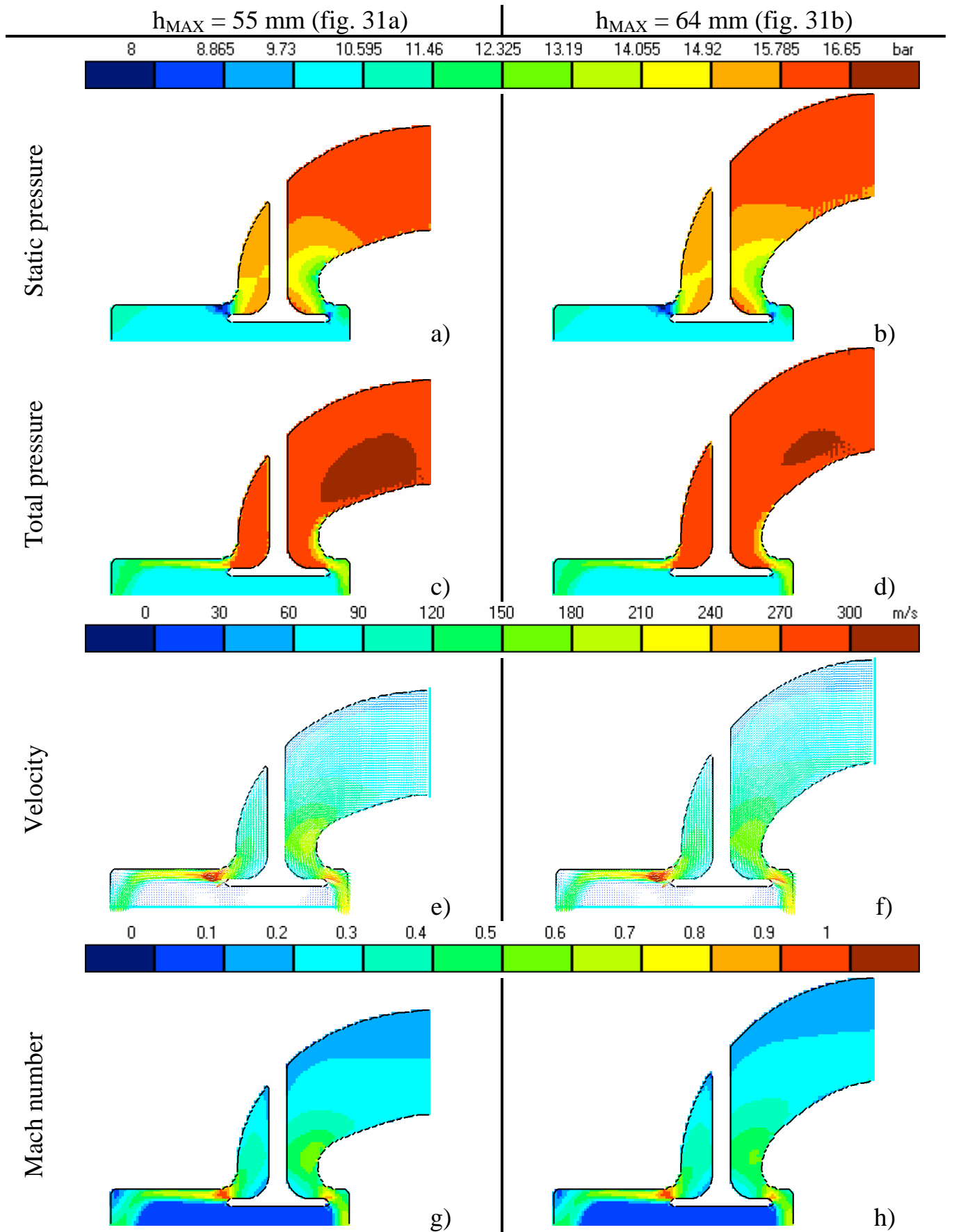


Fig. 32. Gas flow parameters at different position of the upper edge of the port roof

7 variants of inlet port area were considered, fig. 33. The larger the inlet area of the port the larger air mass flow, fig. 34. However the value $A_{INL}=14 \text{ cm}^2$ seems as optimal. The calculated fields of velocities, Mach number, static pressure and total pressure are presented in the figure 35 for different variants of intake port inlet area.

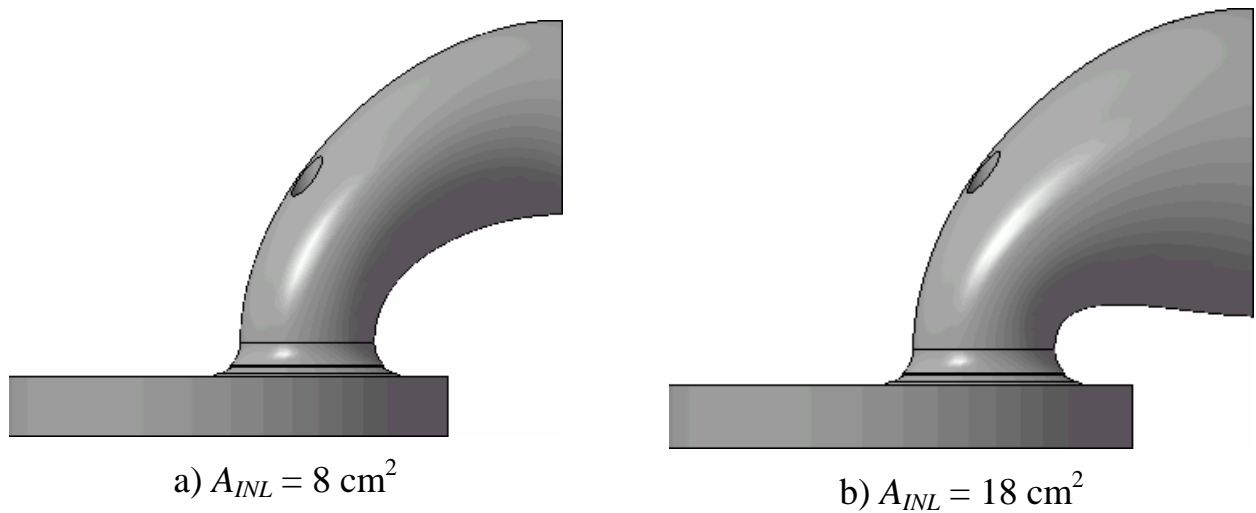


Fig. 33. Intake ports with a different cross section area of the port inlet

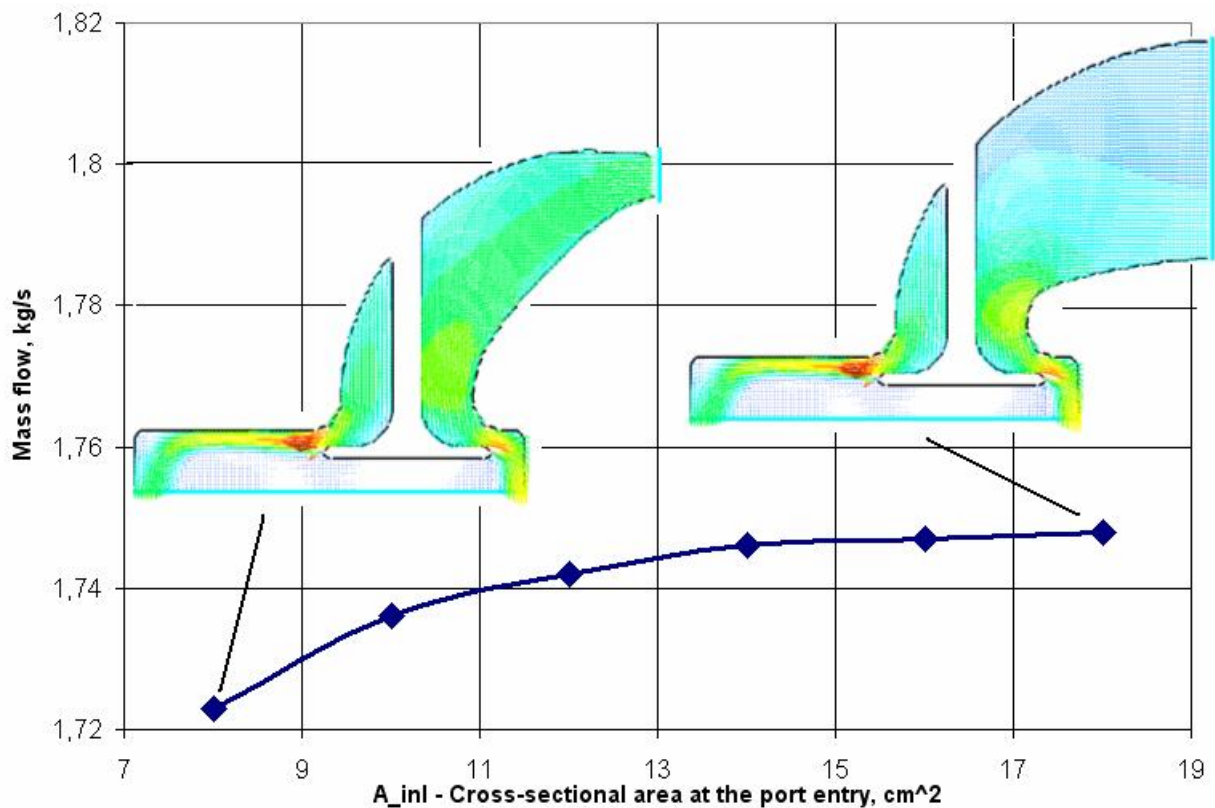


Fig. 34. Effect of cross section area of the port inlet on the mass flow.

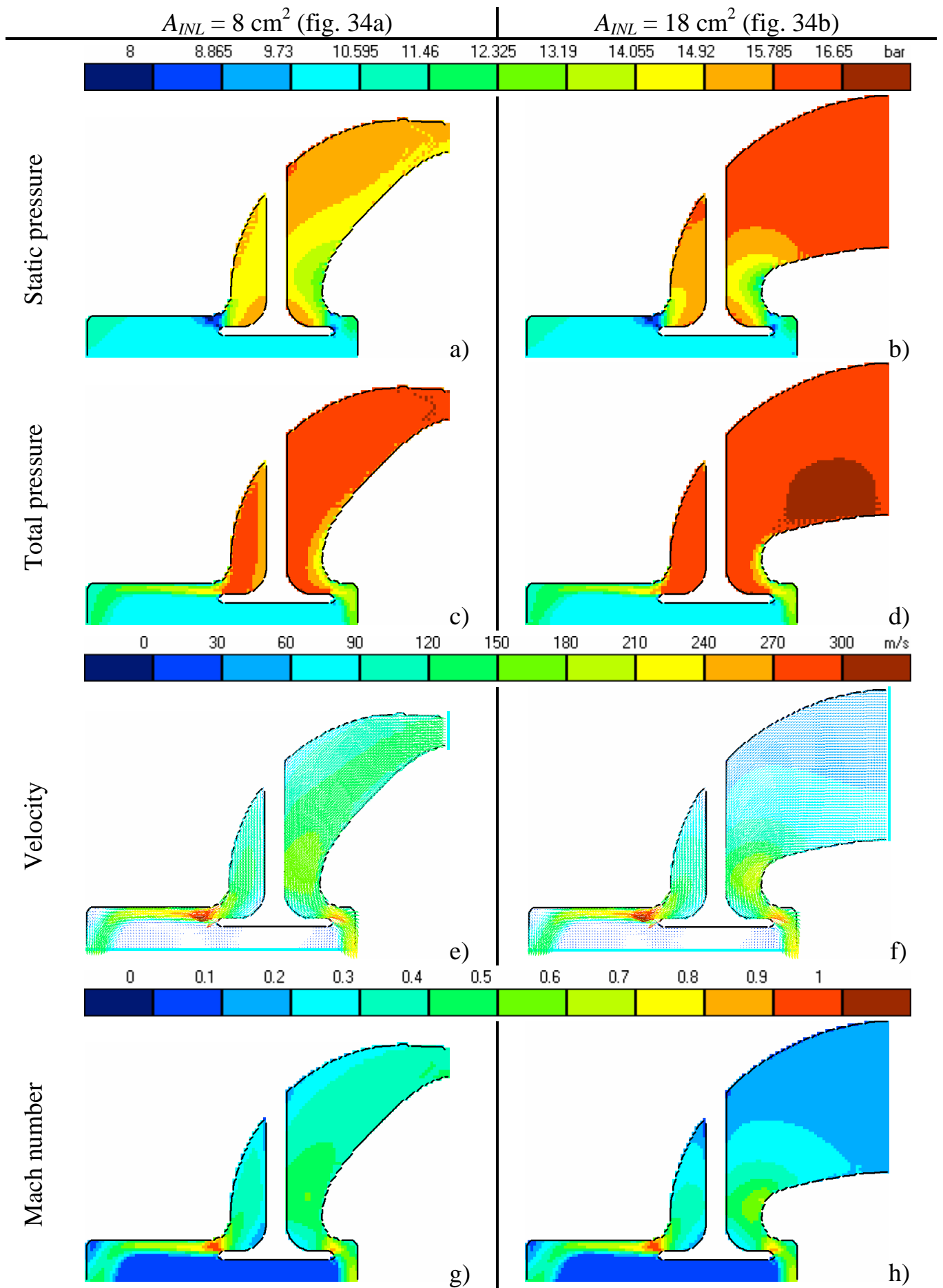


Fig. 35. Cross-section area at the port entry effect

A valve head diameter has a very strong effect on mass flow. But, a big valve produces an irregular velocity field due to closely placed another valve or cylinder wall. In the investigated diapason of valve head diameter variation the positive effect of large flow area exceed negative effect of encumbering of flow area by neighbour valve and cylinder wall, fig. 36. 3D domain is presented in the fig. 37. Flow parameters are shown in fig.38. The $D_v=28$ mm was fixed as optimal solution due to account of exhaust valve.

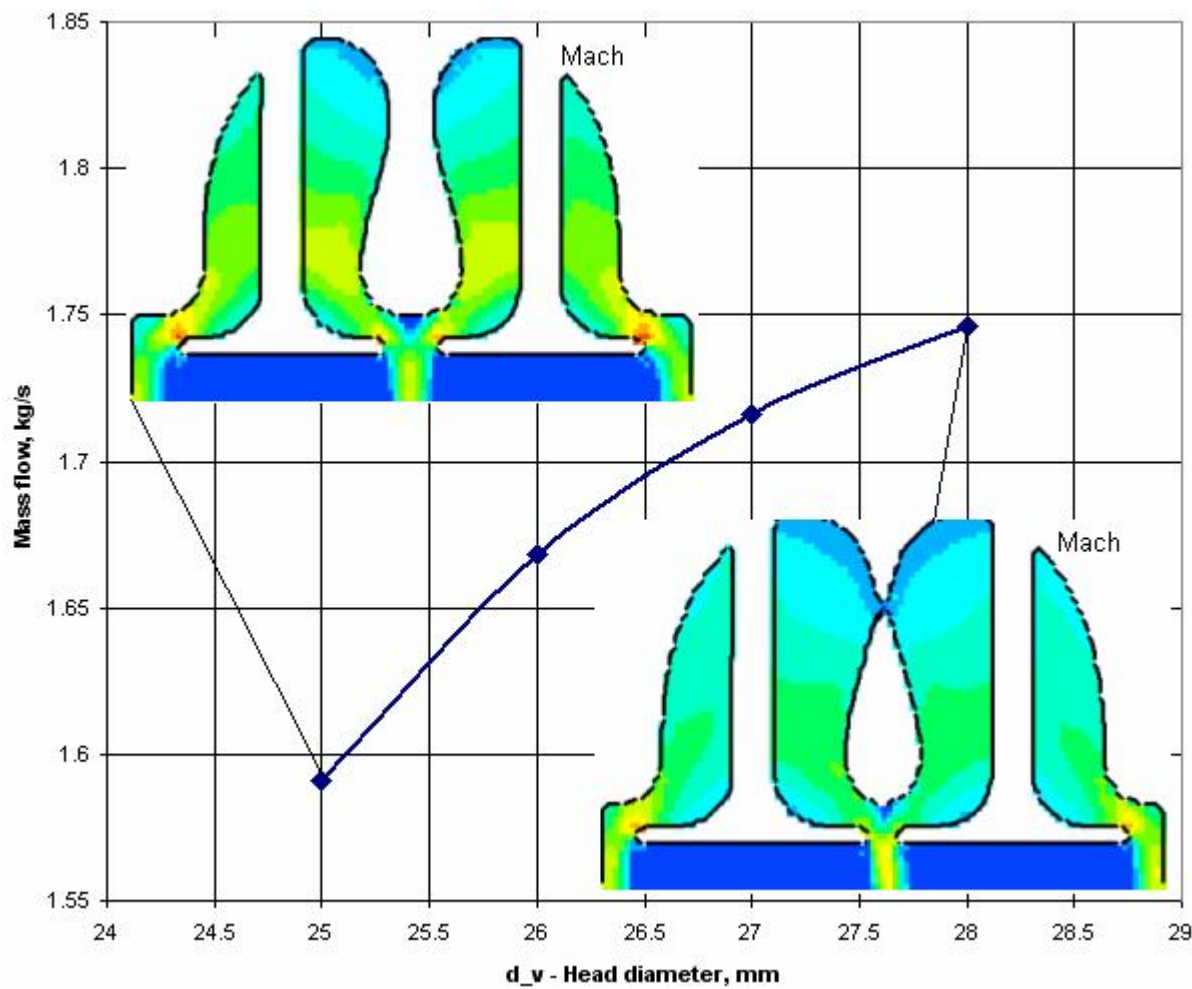


Fig. 36. Dependence of the mass flow on the valve head diameter

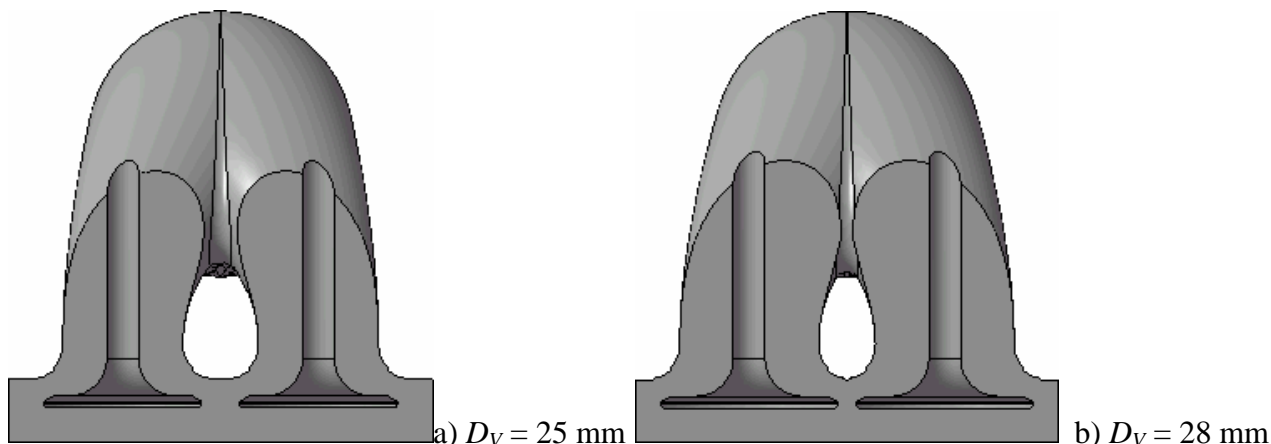


Fig. 37. Intake port at different valve head diameter.

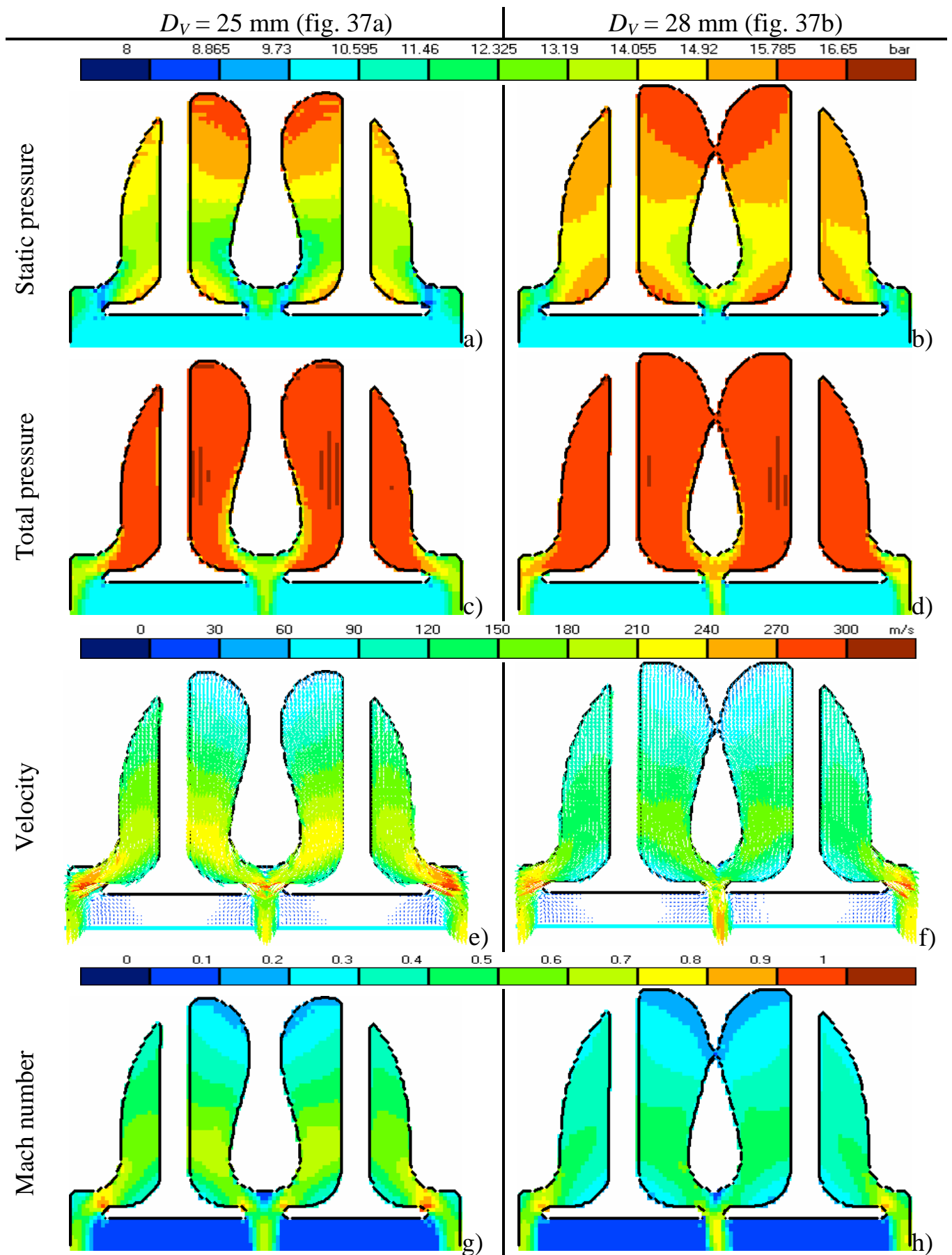


Fig. 38. Gas flow parameters at different valve head diameter D_V .

The distance from cylinder axis to the plane of the intake valves axis named as x_v was varied from 7 mm up to 13 mm, fig. 39. The x_v has significant effect in mass flow, fig. 40. The effect is caused by encumbering of flow area by neighbour cylinder wall. The more distance from cylinder wall the larger air flow. The optimum value is $x_v = 10$ mm (if it allows an exhaust ports design). Flow parameters for the cases of $x_v = 7$ mm and $x_v = 13$ mm are shown in fig.41.

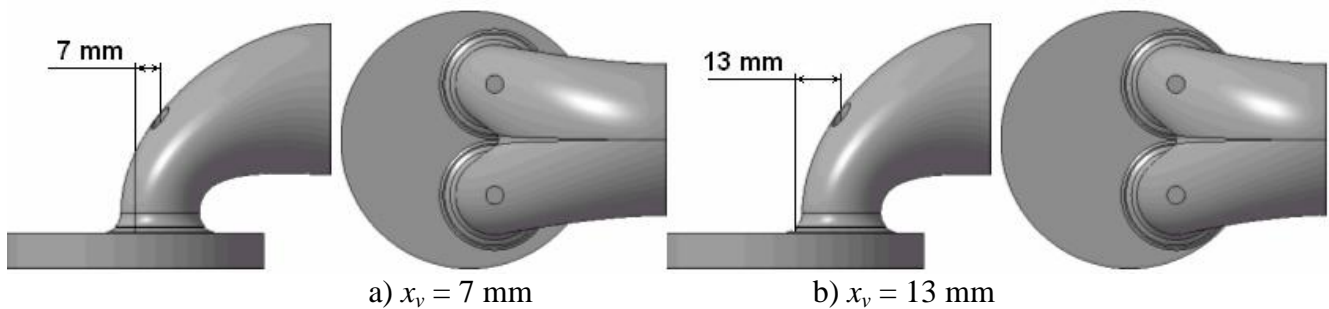


Fig. 39. 3D Intake port domain at different distance from cylinder axis to the plane of the intake valves axis

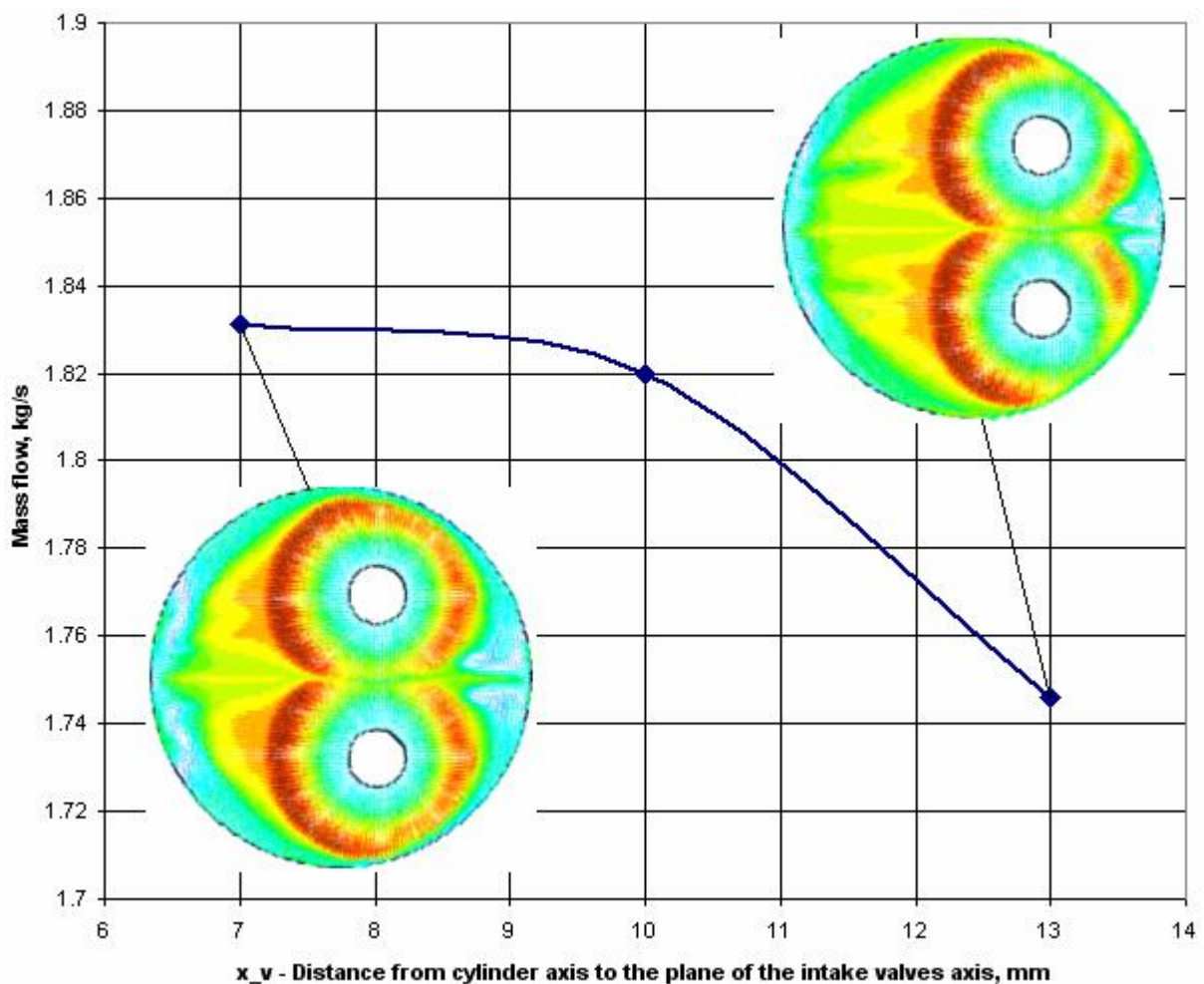


Fig. 40. Effect of distance x_v on the mass flow

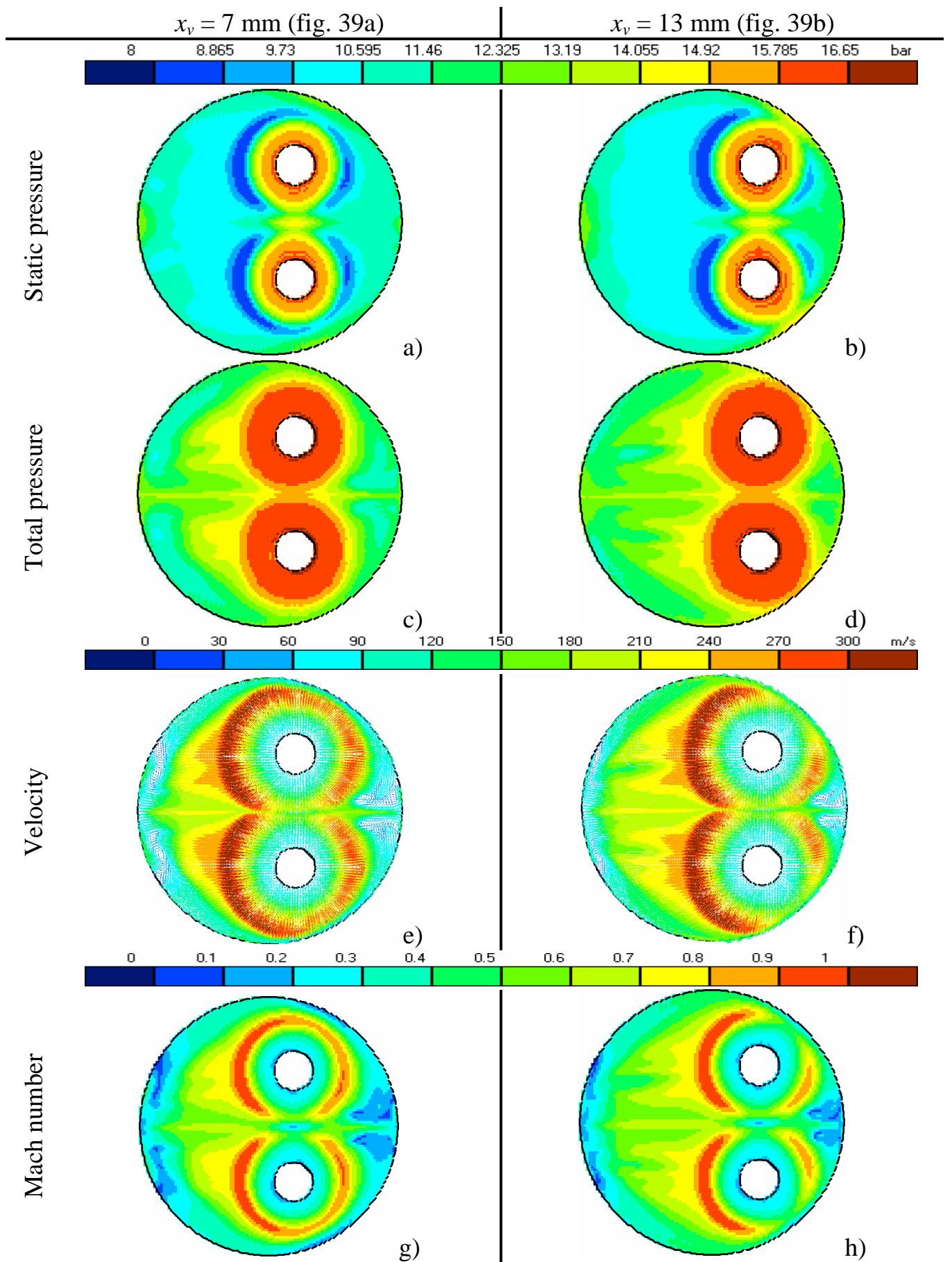


Fig. 41. Flow parameters at different x_v .

The configuration of the z-engine intake ports being obtained as a result of optimization is presented in the figure 42.

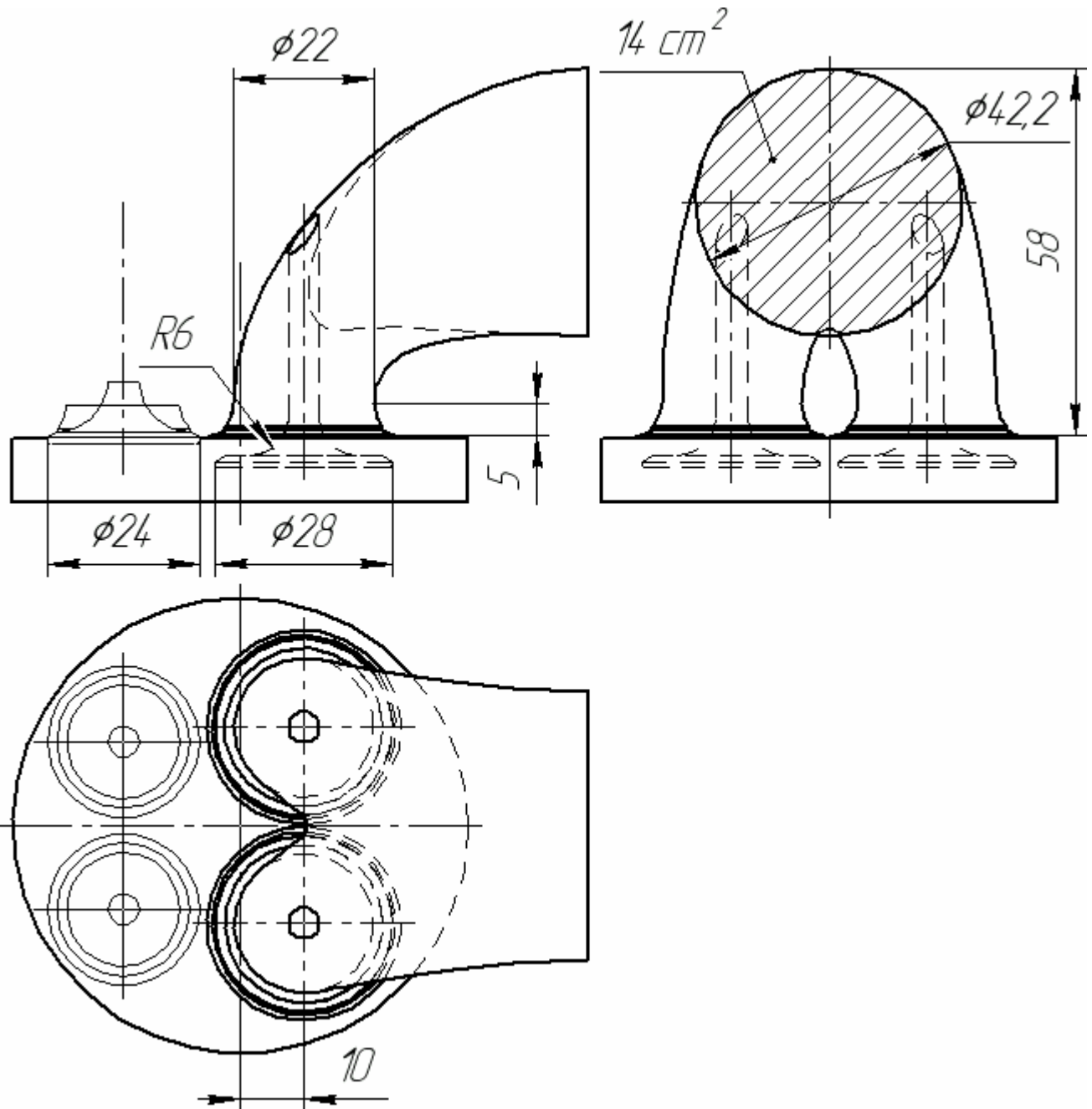


Fig. 42. Sketch of the recommended intake port of the z-engine.

The air flow parameters corresponded with optimized port configuration are presented in APPENDIX in figures: 49, 50, 51, 52.

6. Discharge coefficient for thermodynamic engine simulation

After the intake port dimensions optimization there was calculated discharge coefficient C_d of the ports to be used in thermodynamic engine simulations and port timing optimization being done with DIESEL-RK software. The well known expression for port effective flow area calculation was used [3]:

$$A_{int} = n_v \pi D_v L_v C_d; \quad (1)$$

where: $n_v = 2$ is number of intake valves per cylinder, D_v is a valve head diameter, $L_v = f(CA)$ is a current valve lift, $C_d = f(L_v / D_v)$ is a discharge coefficient depending on valve lift rated to D_v . On the another hand the effective flow area may be defined from theoretical and real air mass flow m_{air} , where theoretical mass flow is calculated from Bernoulli equation and real mass flow is calculated with CFD:

$$A_{int} = \frac{m_{air}}{\sqrt{p_1 r_1 \frac{2g}{g-1} \left[\left(\frac{p_2}{p_1} \right)^{\frac{2}{g}} - \left(\frac{p_2}{p_1} \right)^{\frac{g+1}{g}} \right]}}; \quad (2)$$

where p_1 and r_1 are pressure and density of air before intake port, p_2 is pressure in cylinder, g is adiabatic exponent. Discharge coefficient C_d was calculated for different values of the valve lift in optimized intake port at few levels of pressure ratios:

- $p_1 = 16.6$ bar; $p_2 = 9.9$ bar: to obtain actual C_d for specific z-engine conditions.
- $p_1 = 1.1$ bar; $p_2 = 1.0$ bar: to obtain typical C_d function and verify CFD simulation at typical conditions.
- $p_1 = 16.6$ bar; $p_2 = 15$ bar at $L_v / D_v = 0.15$: to check correctness of an assumption about usability of typical C_d function at high intake pressure (~15 bar). If usability will be confirmed the typical C_d function can be used.

The typical C_d function [3, 4] is presented in fig. 43 by green curve, the C_d function obtained for the z-engine optimized inlet port with a small pressure ratio is shown by magenta curve, the same C_d function but obtained for large pressure ration is plotted by dark blue curve. An comparison of the curves shows quite well agreement of Annand & Roe curve with C_d function calculated here. A difference in C_d at the small valve lift

($L_v / D_v < 0.05$) takes place due to different angle of seat face. The popped valve with 30° seat face should have a larger geometrical flow area at the small valve lift; the An-nand & Roe curve was obtained for 45° seat face.

The significant difference between dark blue and magenta curves says about necessity to take into account the dependence of discharge coefficient on the pressure ratio if pressure ratio is quite large (here one reaches 1.67) and on total value of the pressure.

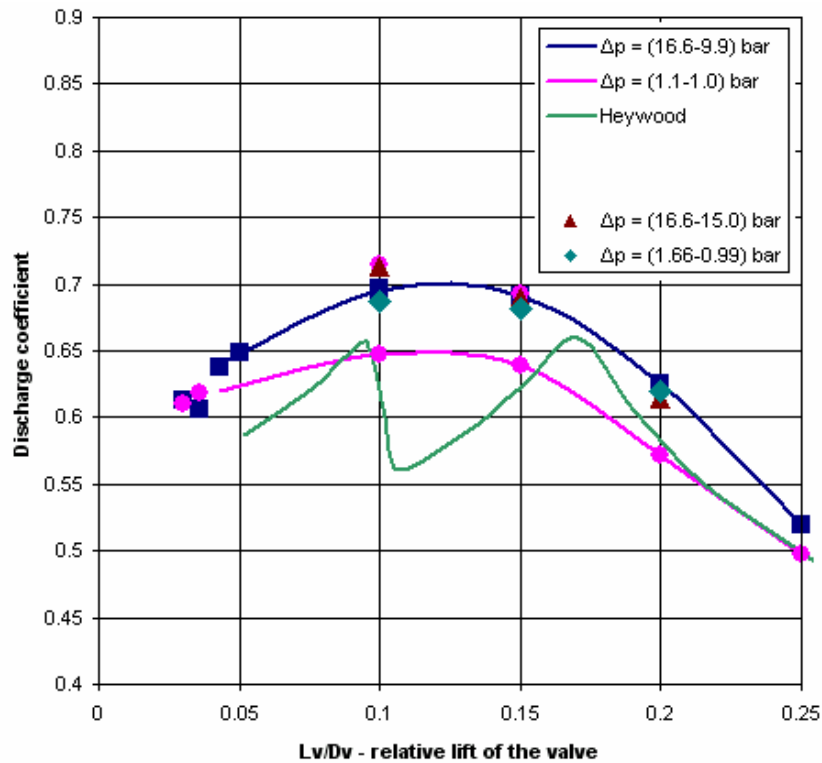


Fig. 43. Discharge coefficient as a function of relative valve lift

Simulations of the flow in the z-engine intake port were done also for small pressure ratio and high pressure level (brown triangles \blacktriangle) and for high pressure ratio and small pressure level (green rhombs \blacklozenge). Everywhere the inlet pressure rise results in discharge coefficient increasing. This conclusion may be confirmed (by indirection) with data presented by Heywood [3] for two stroke engine, fig. 44, where discharge coefficient increases significantly at inlet pressure rise.

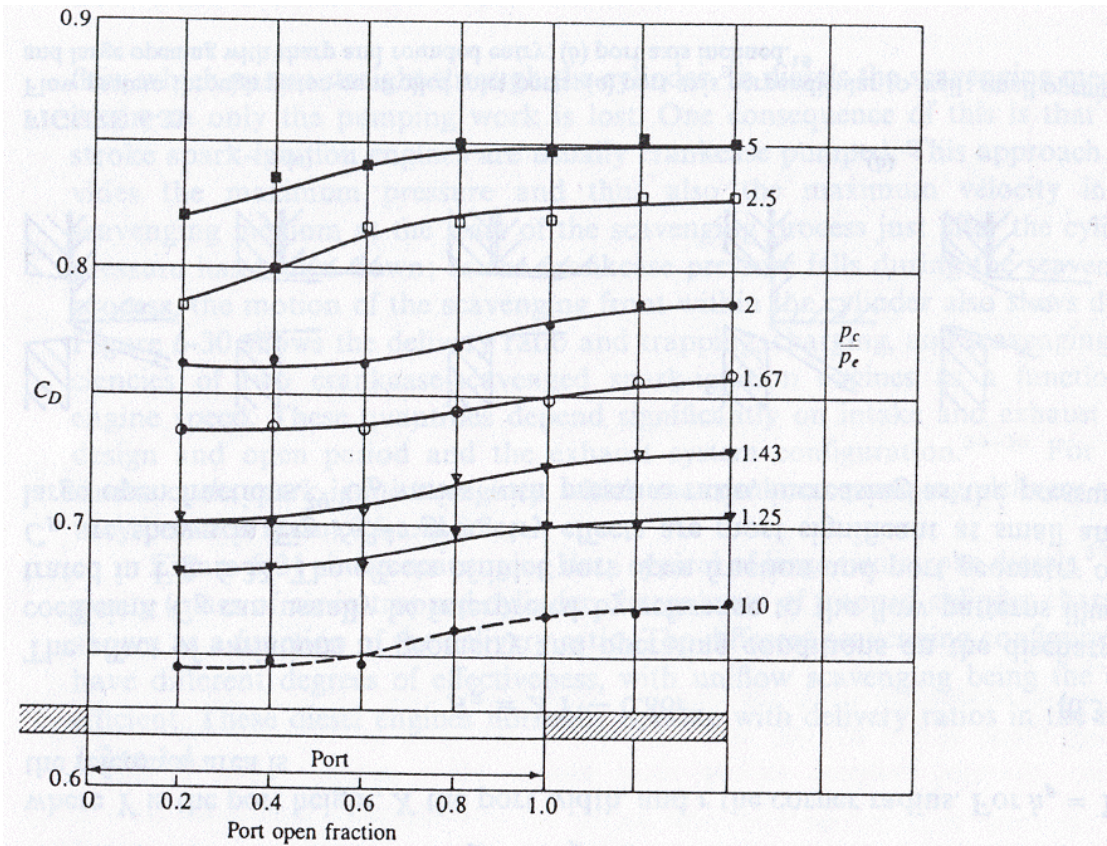


FIGURE 6-36
 Discharge coefficient of a single rectangular exhaust port (7.6 mm wide \times 12.7 mm high) in the wall of a 51-mm bore cylinder as a function of open fraction and pressure ratio. Steady-flow rig tests at 21°C. p_c = cylinder pressure, p_e = exhaust system pressure.³⁹

Fig. 44. Discharge coefficient as a function of port open fraction and pressure before port.

7. Thermodynamic z-engine simulation with obtained intake port discharge coefficient

As it shown in the figure 43, the discharge coefficient C_d is larger at the large pressure difference between intake and cylinder (blue curve) and at large pressure level before and after a valve. This takes place at whole period of the z-engine intake valves open. So the blue curve was used at the specification of effective flow area diagram. There was used following expression for effective flow area:

$$A_{int} = MIN \left\{ \begin{array}{l} 2p D_v L_v C_d; \\ 2 \frac{p}{4} (D_t^2 - D_s^2) C_{dth} \end{array} \right\}; \quad (3)$$

where: C_d is discharge coefficient for valve curtain area (fig. 43); $D_v = 2.8$ cm is a valve head diameter; $D_t = 2.2$ cm and $D_s = 0.5$ cm are throat diameter and steam diameter, $C_{dth} = 0.8$ is discharge coefficient for throat area. The equation includes valve curtain area part and port throat area part. The values of A_{int} corresponding with fixed ratios: $L_v / D_v = 0; 0.043; 0.1; 0.15; 0.02$ are presented in the figure 45. Maximum effective flow area takes place in the port throat when valve lift L_v is quite big, this value is shown by magenta curves in the fig. 45.

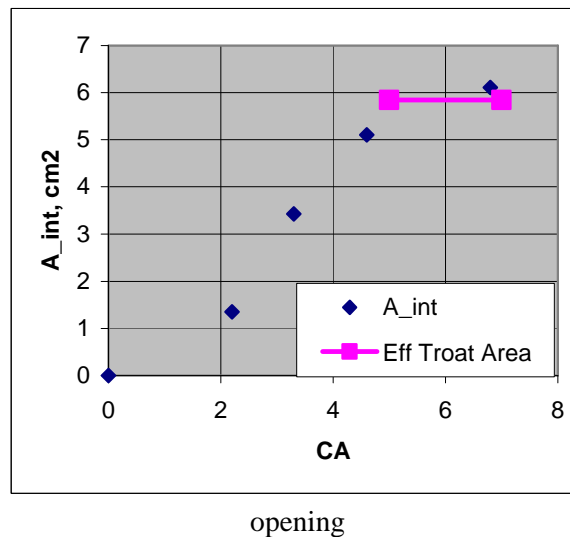
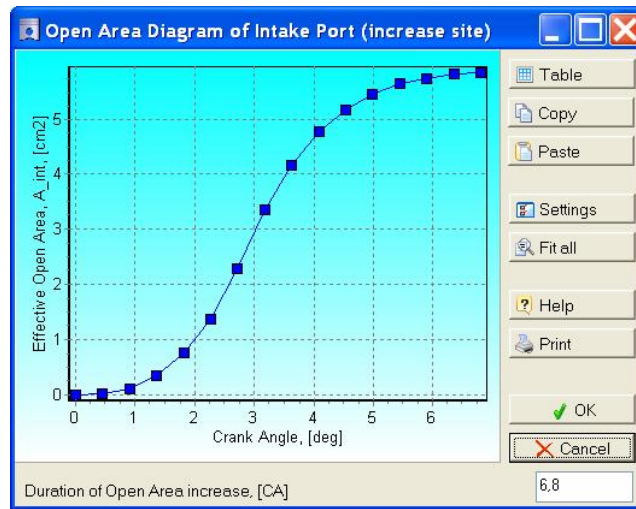


Fig. 45. Effective flow area corresponding with fixed ratios of valve lift to valve head diameter: $L_v / D_v = 0; 0.043; 0.1; 0.15; 0.02$ for opening and closing phases.

At the developing diagram of fig. 45 there was assumed the valve lift is 5.6 mm may be reached during 6.8 CA deg. The valve lift profile is close to sine function. The

obtained rare points of fig. 45 were complement to describe precisely the effective flow area of port during opening and closing to be used in DIESEL-RK for thermodynamic cycle simulation. The results are shown in the fig. 46. Duration of valve opening was optimized to achieve a best fuel consumption and maximum Air/Fuel ratio, fig. 46.



opening

Fig. 46. Effective flow area for opening and closing phases of intake valve motion.

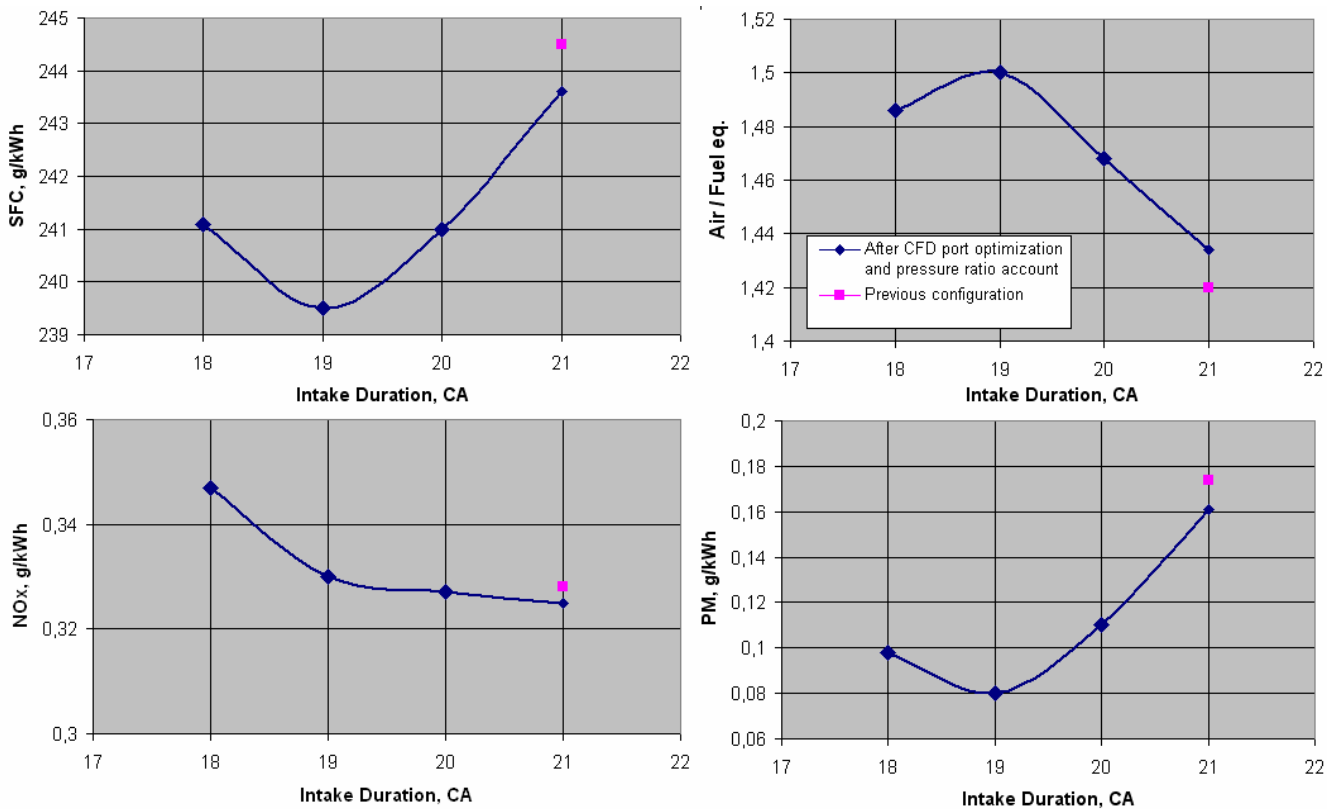


Fig. 47. Effect of intake duration on z-engine parameters.

Analysis of fig. 47 shows the best duration of intake is 19 CA deg. One allows decrease fuel consumption in 4 g/kWh, decrease PM emission and increase Lambda.

NOx stills same. Parameters of gasexchange at optimal point are presented in the fig. 48 in comparison with ones being character for previous configuration having duration of intake: 21 CA deg.

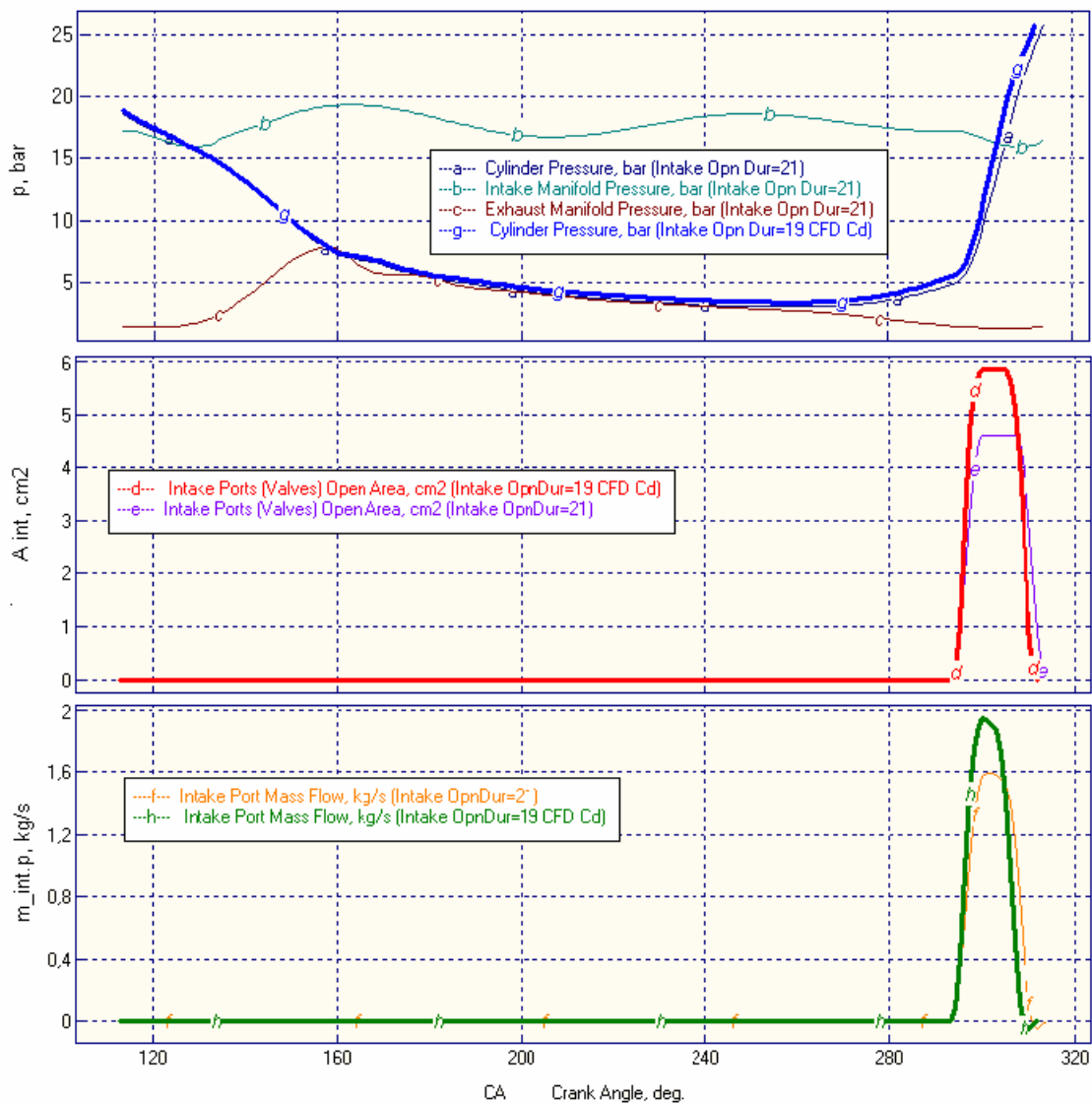


Fig. 48. Gasexchange of z-engine at maximum power point with optimal intake duration (19 CA deg.)

The analysis of the obtained results shows more efficient intake with optimized intake port. It allows decreasing the SFC in 4 g/kW h with decreasing the PM emission. The z-engine is very sensitive to the intake process at the large power points. It is necessary to design the intake ports of engine so to provide maximum effective flow area and fast valve opening till 5.6 mm during 6.8 CA deg. at 3600 RPM.

8. Conclusion

1. The greatest effect on the mass flow through the intake ports have:

- a valve head diameter D_v ;
- a distance from cylinder axis to the plane of the intake valves axis x_v .

The less x_v the more equability of filling the gap around the valve head (see Fig. 41 e, f, g, h). The same effect of equability can be achieved by decreasing the diameters of the valve head, but due to the reduced flow area the mass flow decreases, so the inlet valve should be made with maximum possible diameter. Other geometrical characteristics of the port (assuming a smooth change in flow area and the lack of sharp ledges in it) affect the flow not much. The fillet radius of the valve is recommended to perform not more than 8 mm, the cross-sectional area at the port inlet must be at least 14 cm². The lifting of the upper edge of the port roof has a positive effect on the flow through the ports but an increase an engine dimensions calls into question this decision.

The specific dimensions of the proposed port are shown in fig. 42.

2. There was obtained discharge coefficient of the engine intake port as a function of valve lift for conventional conditions of small difference of pressure (1.1-1.0 bar) and for specific conditions of large difference of pressure (16.6-9.9 bar), fig. 43. The discharge coefficient functions are intended for use in thermodynamic engine simulation tools. The discharge coefficient for large pressure drop has to be used for simulation of the gas exchange of z-engine.

3. The optimum duration of intake is 19 CA deg. (the full load point @ 3600 RPM). The obtained solution allows decrease fuel consumption in 4 g/kWh, decrease PM emission and increase Lambda. NOx stills same.

References

1. www.diesel-rk.bmstu.ru

2. Grishin Yu.A. A new schemes of large particles method and their use for engine gasexchange systems optimization // Mathematical Modelling. 2002, Vol. 14, No 8, pp. 51-55. (in Russian). Гришин Ю.А. Новые схемы метода крупных частиц и их использование для оптимизации газоздушных трактов двигателей // Математическое моделирование. 2002, т. 14, №8, с.51-55.

3. Heywood, J.B.: Internal Combustion Engine Fundamentals, McGraw-Hill, New York, 1988.

4. Annand, W.J.D., and Roe, G.E.: Gas Flow in the Internal Combustion Engine, Haessner Publishing, Newfoundland, NJ., 1974.

Appendix

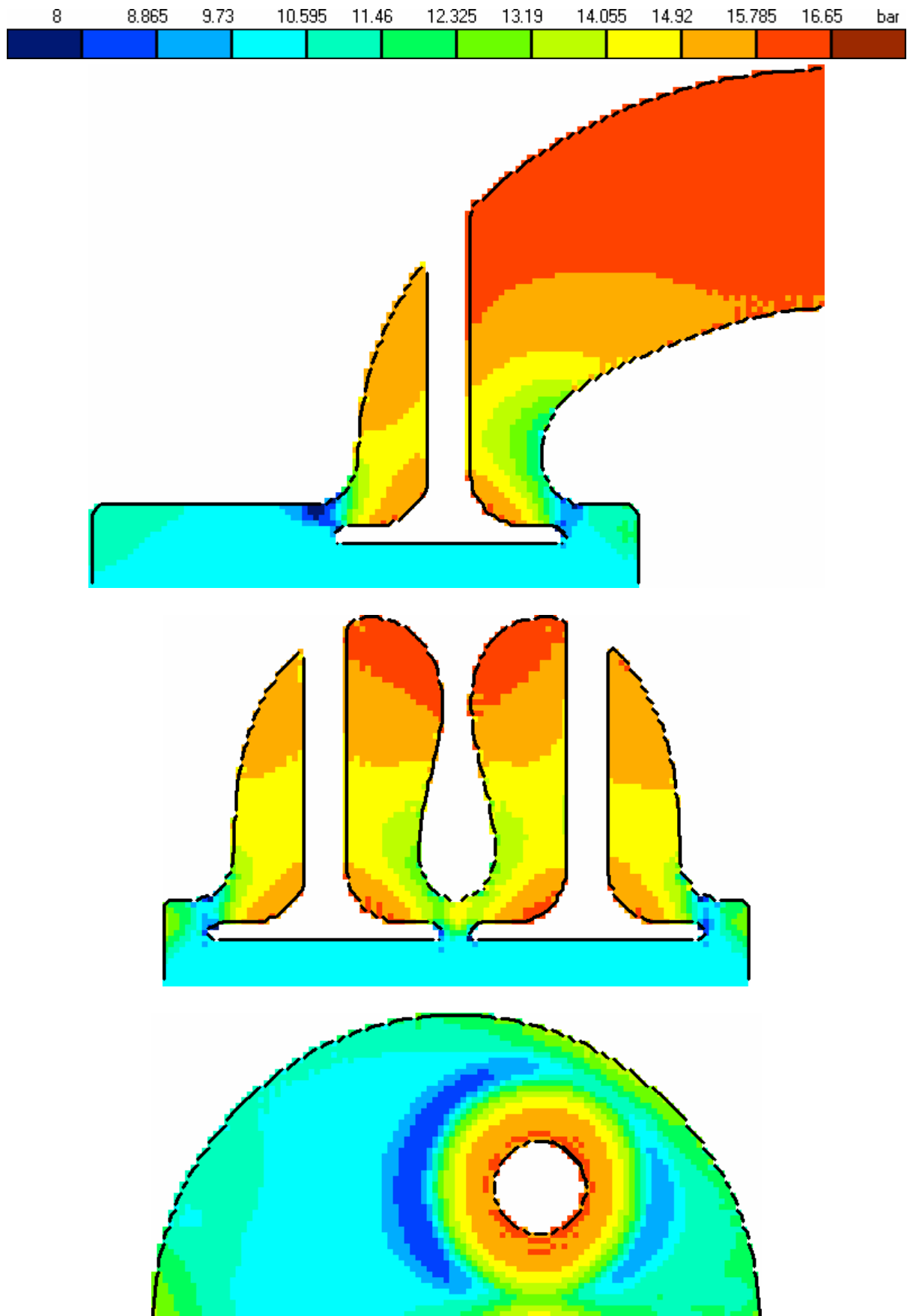


Fig. 49. The field of static pressure in three sections of optimized intake port

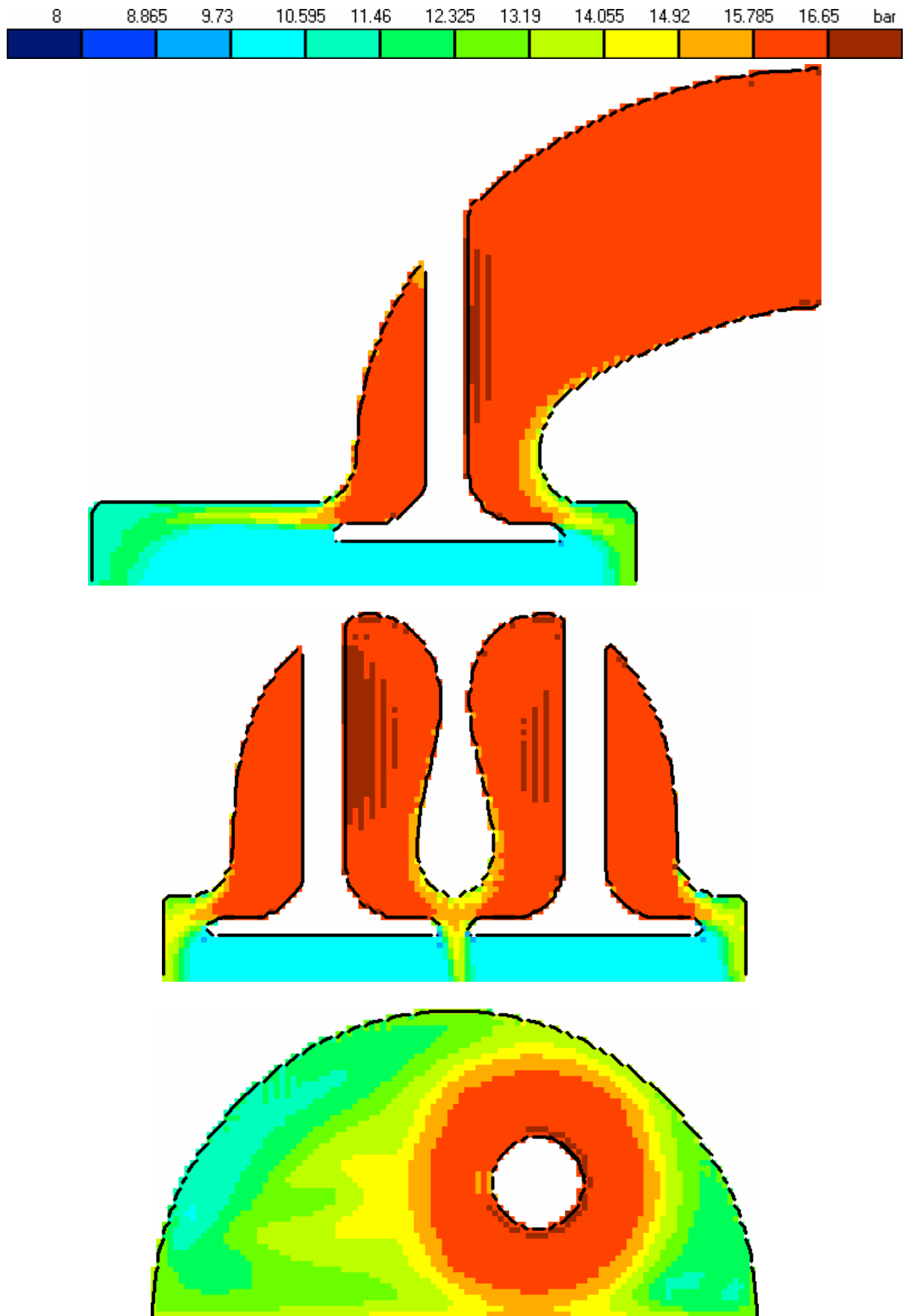


Fig. 50. The field of total pressure in three sections of optimized intake port

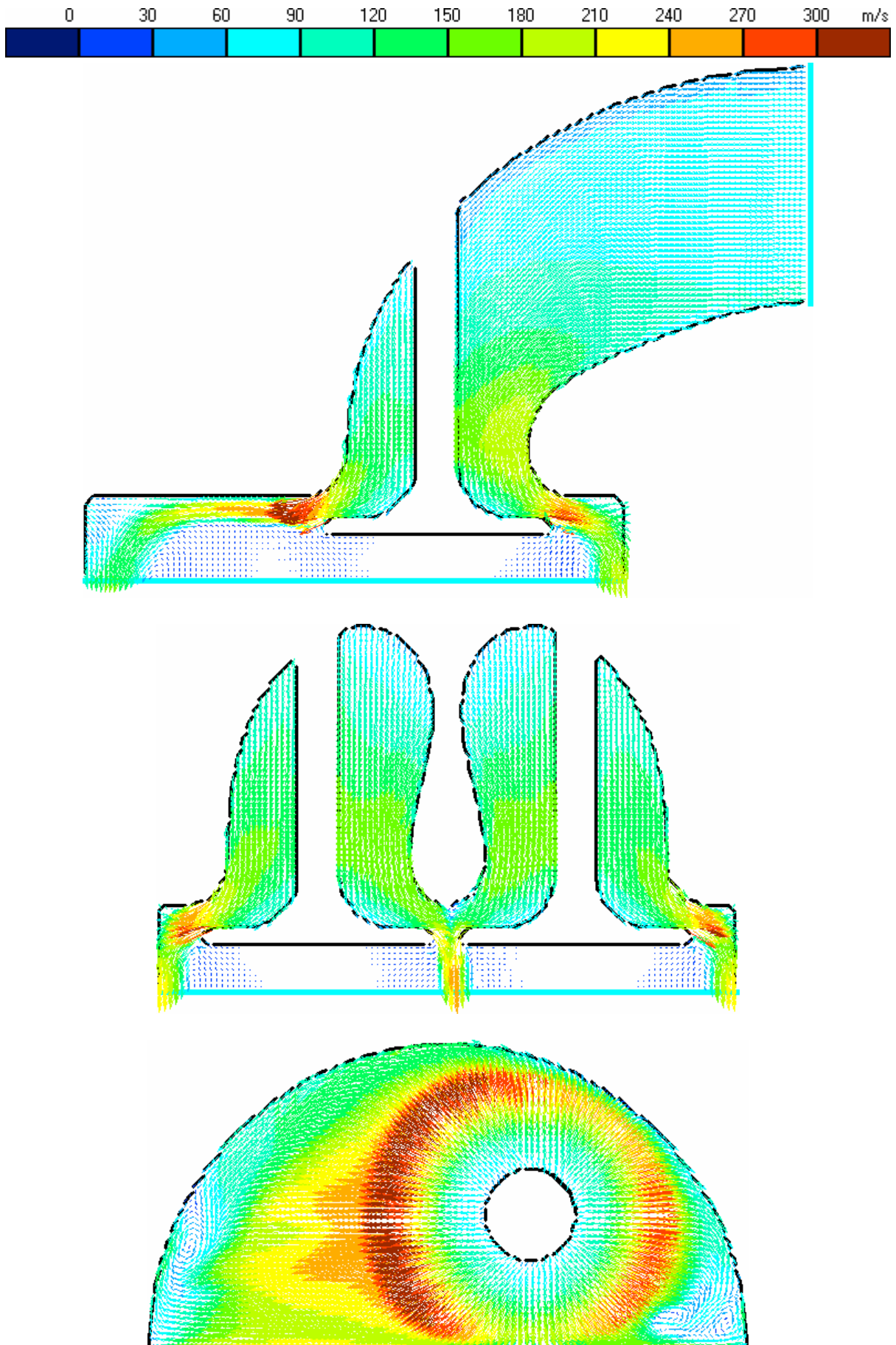


Fig. 51. The field of velocity in three sections of optimized intake port

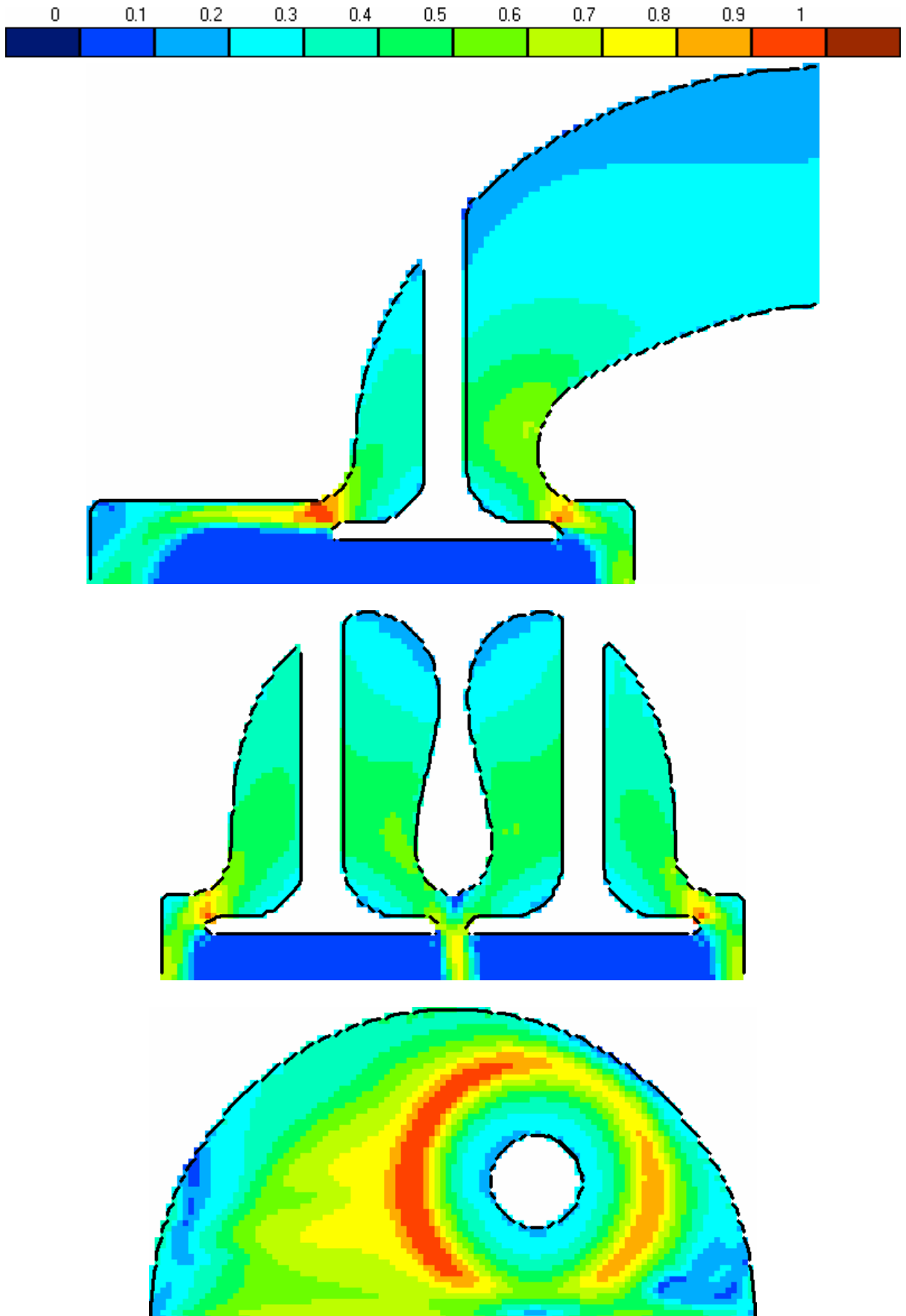


Fig. 52. The field of Mach number in three sections of optimized intake port